# Ground-state and collective modes of a spin-polarized dipolar Bose-Einstein condensate in a harmonic trap

I. Sapina, T. Dahm, and N. Schopohl*
*Institut für Theoretische Physik and Center for Collective Quantum Phenomena, Universität Tübingen, Auf der Morgenstelle 14, D-72076 Tübingen, Germany*
(Received 24 June 2010; published 18 November 2010)

We report results for the Thomas-Fermi ground state of a spin-polarized dipolar interacting Bose-Einstein condensate for the case when the external magnetic field **B** is not orientated parallel to a principal axis but is aligned parallel to a symmetry plane of a harmonic anisotropic trap. For a dipole interaction strength parameter $\varepsilon_D \neq 0$ the release energy of the condensate depends on the trap orientation angle $\vartheta_T$ between the principal axis $\mathbf{e}_{z,T}$ of the trap and the field **B**. From the quasiclassical Josephson equation of macroscopic quantum physics we determine the low-lying eigenfrequencies of small-amplitude collective modes of the condensate density for various trap frequencies $\omega_a$ and trap orientation angles $\vartheta_T$. For the special case of a *spherical* harmonic trap with trap frequency $\omega$ it is rigorously shown for $-\frac{1}{2} < \varepsilon_D < 1$ that a pure $s$-wave symmetry breather excitation of the condensate density exists, that oscillates at a constant frequency $\Omega_s = \sqrt{5}\omega$ around the ground-state cloud, despite the well-known fact that the shape of the ground-state cloud of a spin-polarized dipolar condensate is for $\varepsilon_D \neq 0$ not isotropic. For $\vartheta_T \neq 0$ the small-amplitude modes of the particle density with isotropic and quadrupolar symmetry consist of two groups. There exist four modes that are combinations of basis functions, with $s$-wave, $d_{x^2-y^2}$- and $d_{z^2}$-wave, and $d_{xz}$-wave symmetry, and two modes that are combinations of basis functions with $d_{yz}$- and $d_{xy}$-wave symmetry. A characteristic difference in the dependence of the frequencies of these six collective modes on the dipole interaction strength parameter $\varepsilon_D$ for prolate and oblate harmonic triaxial traps, respectively, is suggested to be used as an experimental method to measure the $s$-wave scattering length $a_s$ of the atoms.

DOI: 10.1103/PhysRevA.82.053620 PACS number(s): 67.85.Hj, 03.75.Hh, 03.75.Kk

## I. INTRODUCTION

Experiments with trapped, extremely dilute gas clouds, consisting of identical atoms with mass $m^\star$, and forming at ultracold temperatures a quantum degenerate Bose-Einstein condensate (BEC), are nowadays a research focus in many laboratories. It was realized early that cold atom clouds do not form an ideal Bose gas but experience *isotropic* interaction forces in the low-energy sector of the system that can be well described by a microscopic $s$-wave scattering length $a_s$ [1]. While the size of an ideal Bose gas confined inside a *harmonic* trap with trap frequency $\omega$ is determined by the width $a_\omega = \sqrt{\frac{\hbar}{m^\star\omega}}$ of the ground-state wave function of a single particle, the size of an *interacting* cold atom cloud consisting of a large number $N \gg 1$ of condensed Bose atoms may increase to much larger distances, $\Lambda_{\mathrm{TF}} = a_\omega(\frac{4\pi N a_s}{a_\omega})^{\frac{1}{5}}$. Fortunately, the necessary requirement, $\frac{4\pi N a_s}{a_\omega} \gg 1$, for observing a BEC in a harmonic trap can be realized simultaneously with the condition of a small diluteness parameter $n_0 a_s^3 \ll 1$, so the mean-field theory of Ginzburg and Pitaevskii for interacting Bose systems is applicable for a wide range of parameters, $a_\omega$ and $a_s$. As the length $\Lambda_{\mathrm{TF}}$ increases with increasing $N$, the kinetic energy $E_K \simeq \frac{\hbar^2}{2m^\star\Lambda_{\mathrm{TF}}^2}$ of the interacting particles in the ground state eventually becomes much smaller than the potential energy $V_T \simeq \frac{m^\star}{2}\omega^2\Lambda_{\mathrm{TF}}^2$ of the particles, because the density inside the BEC becomes a smooth and slowly varying function of position. In the Thomas-Fermi approximation the kinetic energy term for the particles in the ground state of the BEC is neglected altogether. This is justified when the chemical potential $\mu$ of the interacting system is much larger than the chemical potential $\sim \frac{3}{2}\hbar\omega$ of the noninteracting Bose gas. So for $\frac{4\pi N a_s}{a_\omega} \gg 1$ the dominant balance required for mechanical equilibrium of a trapped BEC is between the repulsive interactions of the atoms and the confinement forces of the trap.

Interesting physics can be observed when, in addition to the usual $s$-wave contact interaction, the atoms are influenced by long-range dipole-dipole forces [2]. This occurs, for example, for Bose atoms with nuclear spin $I = 0$ and integer (electronic) spin $S$, thus giving rise to a multiplet $-S \leqslant M_S \leqslant S$ of atomic magnetic dipole moments with the $z$ component $2\mu_B M_S$. A transition metal atom like chromium $^{52}$Cr has $I = 0$ and $S = 3$. On the other hand, alkali-metal atoms like $^{87}$Rb carry (nuclear) spin $I = \frac{3}{2}$ and $S = \frac{1}{2}$, thus coupling to a total spin $F = 1$ in the lowest energy state. The first experimental study of magnetic dipole-dipole interactions in a BEC was realized with $^{52}$Cr atoms [3] carrying a large magnetic moment $|\langle\mathbf{M}\rangle| = 6\mu_B$. A quantum degenerate $F = 1$ spinor BEC was synthesized successfully with $^{87}$Rb atoms [4]. Recently, intrinsically anisotropic BEC systems with electric dipole-dipole interactions between polar molecules have been studied experimentally [5]. New research directions are concerned with magnetic quantum gases consisting of heavy rare-earth-metal atoms like thulium [6] with $|\langle\mathbf{M}\rangle| = 4\mu_B$, erbium [7] with $|\langle\mathbf{M}\rangle| = 7\mu_B$, and dysprosium [8] with $|\langle\mathbf{M}\rangle| = 10\mu_B$.

*nils.schopohl@uni-tuebingen.de

 

In the ensuing considerations we study spin-polarized Bose atom clouds. When the magnetic dipole moments of the atoms are 100% polarized under a homogeneous external magnetic induction field $\mathbf{B} = B^{(\mathrm{ext})}\mathbf{e}_z$, so all atoms in the cold gas cloud carry the identical effective magnetic moment, say, $\langle \mathbf{M} \rangle = -2\mu_B S\,\mathbf{e}_z$, it is still possible to describe the Bose-condensed ground state $\Psi$ of $N$ interacting atoms by a *scalar* Hartree ansatz:

$$\Psi(\mathbf{r}^{(1)},\ldots,\mathbf{r}^{(N)}) = \psi(\mathbf{r}^{(1)})\psi(\mathbf{r}^{(2)})\cdots\psi(\mathbf{r}^{(N)}). \qquad (1)$$

The expectation value of the many-body Hamiltonian $H$, evaluated with such a trial wave function $\Psi$ consisting of a product of $N$ identical one-particle wave functions $\psi(\mathbf{r})$, is then minimized with respect to variations of that one-particle wave function $\psi(\mathbf{r})$. The *optimal* one-particle wave function $\psi(\mathbf{r})$ so found is a solution to the Gross-Pitaevskii equation [1]

$$\Big[-\frac{\hbar^2}{2m^\star}\nabla^2_{\mathbf{r}} + V_T(\mathbf{r}) - \mu + (N-1)\int_{\mathbb{R}^3} d^3r'\,U(\mathbf{r},\mathbf{r}')|\psi(\mathbf{r}')|^2\Big]\psi(\mathbf{r}) = 0. \qquad (2)$$

Here, $V_T(\mathbf{r})$ denotes the potential of the trap and $U(\mathbf{r},\mathbf{r}')$ describes the interaction potential between two bosons. The chemical potential $\mu$ is a Lagrange parameter connected to the particle number $N$ in the condensate by the constraint

$$\int_{\mathbb{R}^3} d^3r'|\psi(\mathbf{r}')|^2 = 1. \qquad (3)$$

## II. THOMAS-FERMI THEORY OF SPIN-POLARIZED DIPOLAR BOSE-EINSTEIN CONDENSATE

In the following we investigate the macroscopic quantum degenerate ground state of a spin-polarized system of interacting Bose atoms carrying a magnetic dipole moment $|\langle \mathbf{M} \rangle|$. The interaction potential

$$U(\mathbf{r},\mathbf{r}') = U_0(\mathbf{r},\mathbf{r}') + U_{md}(\mathbf{r},\mathbf{r}') \qquad (4)$$

between two atoms, one at position $\mathbf{r}$ and the other at $\mathbf{r}'$, consists of two contributions, the short-range isotropic $s$-wave interaction pseudopotential

$$U_0(\mathbf{r},\mathbf{r}') = g_s\delta^{(3)}(\mathbf{r}-\mathbf{r}'), \qquad g_s = \frac{4\pi\hbar^2}{m^\star}a_s, \qquad (5)$$

and the long-range *magnetic* dipole-dipole interaction potential

$$U_{md}(\mathbf{r},\mathbf{r}') = \frac{g_{md}}{4\pi}\left[\frac{1}{|\mathbf{r}-\mathbf{r}'|^3} - \frac{3(r_z-r_z')^2}{|\mathbf{r}-\mathbf{r}'|^5}\right], \qquad g_{md} = \mu_0|\langle \mathbf{M}\rangle|^2. \qquad (6)$$

Here the external magnetic induction field $\mathbf{B}$ is orientated parallel to the Cartesian unit vector $\mathbf{e}_z$in the laboratory frame, so the magnetic moments of two interacting atoms, one at positions $\mathbf{r}$ and the other at $\mathbf{r}'$, are both aligned parallel to $\mathbf{e}_z$.

Using well-known identities

$$\frac{3(r_z-r_z')^2}{|\mathbf{r}-\mathbf{r}'|^5} - \frac{1}{|\mathbf{r}-\mathbf{r}'|^3} = \frac{\partial^2}{\partial r_z^2}\frac{1}{|\mathbf{r}-\mathbf{r}'|} - \frac{1}{3}\cdot\nabla^2_{\mathbf{r}}\frac{1}{|\mathbf{r}-\mathbf{r}'|}, \qquad -\nabla^2_{\mathbf{r}}\frac{1}{|\mathbf{r}-\mathbf{r}'|} = 4\pi\delta^{(3)}(\mathbf{r}-\mathbf{r}'), \qquad (7)$$

and introducing the dimensionless parameter [9,10]

$$\varepsilon_D = \frac{g_{md}}{3g_s} = \frac{\mu_0\,|\langle \mathbf{M}\rangle|^2}{\frac{12\pi\hbar^2}{m^\star}a_s} \qquad (8)$$

as a measure of relative strength of magnetic dipole interaction forces, the interaction potential between two atoms in the gas cloud may be rewritten in the guise

$$U(\mathbf{r},\mathbf{r}') = g_s\left[(1-\varepsilon_D)\delta^{(3)}(\mathbf{r}-\mathbf{r}') - 3\varepsilon_D\frac{\partial^2}{\partial r_z^2}\frac{1}{4\pi}\frac{1}{|\mathbf{r}-\mathbf{r}'|}\right]. \qquad (9)$$

In the Thomas-Fermi approximation the particle density profile in the ground state of the trapped BEC

$$n(\mathbf{r}) = |\sqrt{N}\psi(\mathbf{r})|^2 \qquad (10)$$

is a solution to the integral equation

$$(1-\varepsilon_D)n_{\mathrm{TF}}(\mathbf{r}) - 3\varepsilon_D\frac{\partial^2}{\partial r_z^2}\frac{1}{4\pi}\int_{\mathbb{D}_{\mathrm{TF}}} d^3r'\frac{1}{|\mathbf{r}-\mathbf{r}'|}n_{\mathrm{TF}}(\mathbf{r}') = \frac{\mu - V_T(\mathbf{r})}{g_s}. \qquad (11)$$

This is actually a nonlinear problem, because the solution of the integral equation is sought inside the Thomas-Fermi cloud

$$\mathbb{D}_{\mathrm{TF}} = \{\mathbf{r}\in\mathbb{R}^3 | n_{\mathrm{TF}}(\mathbf{r}) \geqslant 0\} \qquad (12)$$

where the region is not known *a priori*. The determination of the shape of the cloud $\mathbb{D}_{\mathrm{TF}}$, or its boundary $\partial\mathbb{D}_{\mathrm{TF}}$, is part of the problem.

Eberlein *et al.* [10] have found for a dipolar interacting BEC confined inside a *harmonic* trap that despite the nonlocal anisotropic dipole-dipole interaction term, the domain $\mathbb{D}_{\mathrm{TF}}$ always maintains the shape of an ellipsoid, as in the case $\varepsilon_D = 0$, but with different semiaxes. We confirm this finding and present additional results for the case when the external magnetic field $\mathbf{B}$ is not in alignment with the principal axis $\mathbf{e}_{z,T}$ of the trap.

Consider a harmonic *anisotropic* trap potential $V_T(\mathbf{r})$ with its minimum at position $\mathbf{r} = \mathbf{0}$ and with the principal axis $\mathbf{e}_{z,T}$ of the trap not in alignment with the field $\mathbf{B}$:

$$V_T(\mathbf{r}) = \frac{m^\star}{2}\left(\omega_x^2 r_{x,T}^2 + \omega_y^2 r_{y,T}^2 + \omega_z^2 r_{z,T}^2\right). \qquad (13)$$

For $\omega_x \neq \omega_y$, $\omega_y \neq \omega_z$, and $\omega_z \neq \omega_x$, surfaces of constant trap potential $V_T(\mathbf{r}) = V_T > 0$ have the geometrical shape of a triaxial ellipsoid. Three mutually orthogonal Cartesian unit vectors $\mathbf{e}_{x,T}$, $\mathbf{e}_{y,T}$, and $\mathbf{e}_{z,T}$ determine the orientation of the principal axes of such a trap. The magnetic field $\mathbf{B}$ is then in general a linear combination of *all* three principal axis vectors: $\mathbf{B} = B_{x,T}\mathbf{e}_{x,T} + B_{y,T}\mathbf{e}_{y,T} + B_{z,T}\mathbf{e}_{z,T}$. For simplicity we restrict our considerations in the following to the special case when the magnetic field $\mathbf{B}$ and the principal axis $\mathbf{e}_{z,T}$

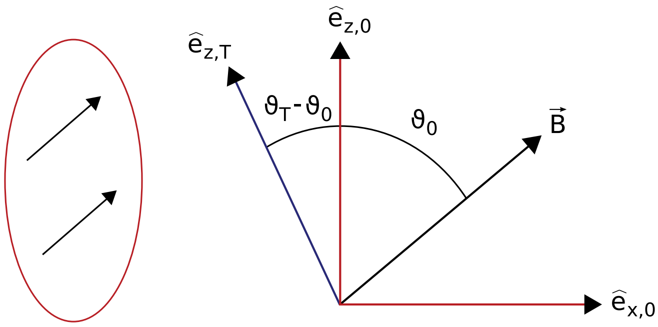


FIG. 1. (Color online) Orientation of principal axis $\mathbf{e}_{z,T}$ of harmonic trap and orientation of principal axis $\mathbf{e}_{z,0}$ of Thomas-Fermi ellipsoid $\mathbb{D}_{\mathrm{TF}}$ relative to the spin polarizing external magnetic field $\mathbf{B}$. The inset on the left-hand side corresponds to a cut of $\mathbb{D}_{\mathrm{TF}}$ with the symmetry plane $y = 0$. Arrows indicate the orientation of the spin-polarizing magnetic field $\mathbf{B}$ relative to the principal axis $\mathbf{e}_{z,0}$ of $\mathbb{D}_{\mathrm{TF}}$.

of the trap span a symmetry plane of the trap, say the plane $r_y = 0$. Then we have in (13)

$$\begin{aligned} r_{x,T} &= r_x(\vartheta_T) = \cos(\vartheta_T) r_x + \sin(\vartheta_T) r_z, \\ r_{y,T} &= r_y(\vartheta_T) = r_y, \\ r_{z,T} &= r_z(\vartheta_T) = -\sin(\vartheta_T) r_x + \cos(\vartheta_T) r_z, \end{aligned} \tag{14}$$

i.e., the principal axis $\mathbf{e}_{z,T}$ of the trap is turned by an angle $\vartheta_T$ around the rotation axes $\mathbf{e}_{y,T} \perp \mathbf{B}$ (see Fig. 1).

As is indicated in Fig. 1, the self-consistent solution of (11) for the density distribution $n_{\mathrm{TF}}(\mathbf{r})$ reveals that the principal axis $\mathbf{e}_{z,0}$ of the Thomas-Fermi cloud $\mathbb{D}_{\mathrm{TF}}$ is rotated away from the direction of the external field by an angle $\vartheta_0 \neq \vartheta_T$. Accordingly, the density profile associated with the ellipsoidal domain $\mathbb{D}_{\mathrm{TF}}$ has the general form

$$n_{\mathrm{TF}}(\mathbf{r}) = n_0 \left(1 - \frac{\tilde{r}_x^2}{\lambda_x^2} - \frac{\tilde{r}_y^2}{\lambda_y^2} - \frac{\tilde{r}_z^2}{\lambda_z^2}\right), \tag{15}$$

where

$$\begin{aligned} r_x(\vartheta_0) &= \tilde{r}_x = \cos(\vartheta_0) r_x + \sin(\vartheta_0) r_z, \\ r_y(\vartheta_0) &= \tilde{r}_y = r_y, \\ r_z(\vartheta_0) &= \tilde{r}_z = -\sin(\vartheta_0) r_x + \cos(\vartheta_0) r_z. \end{aligned} \tag{16}$$

Only in the highly symmetric case $\vartheta_T = 0$ is the principal axis vector $\mathbf{e}_{z,0}$ of the ellipsoid $\mathbb{D}_{\mathrm{TF}}$ orientated parallel to $\mathbf{B}$. For $0 < \vartheta_T < \frac{\pi}{2}$ it is found from the self-consistent solution for the density profile $n_{\mathrm{TF}}(\mathbf{r})$, that $\vartheta_0 \neq \vartheta_T$, i.e., the principal axis $\mathbf{e}_{z,0}$ of $\mathbb{D}_{\mathrm{TF}}$, is never in alignment with the field $\mathbf{B}$, nor is it in alignment with the principal axis $\mathbf{e}_{z,T}$ of the trap (see Fig. 1 and Fig. 2).

The particle density distribution $n_{\mathrm{TF}}(\mathbf{r})$ inside the Thomas-Fermi ellipsoid $\mathbb{D}_{\mathrm{TF}}$ is stratified. Like an onion it consists of a series of thin homoeoidal shells of constant density

$$n_{\mathrm{TF}}(\mathbf{r}) = n_0(1 - \nu^2) = \text{const}, \qquad 0 \leqslant \nu \leqslant 1. \tag{17}$$

Strata of equal density thus correspond to ellipsoidal shells concentric and similar to the bounding ellipsoidal shell $\partial\mathbb{D}_{\mathrm{TF}}$, but with scaled semiaxes $\nu\lambda_a$.

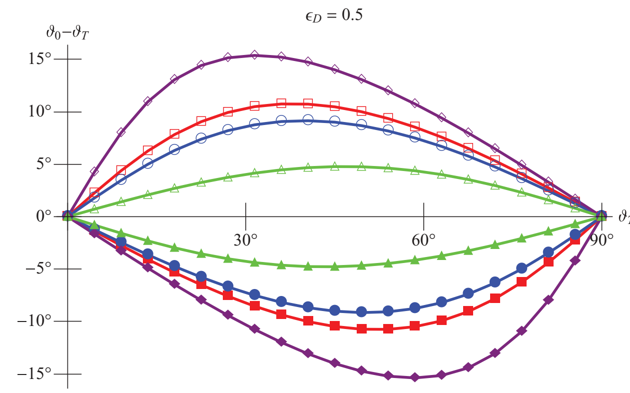


FIG. 2. (Color online) Angle difference $\vartheta_0 - \vartheta_T$ vs trap orientation angle $\vartheta_T$ for the self-consistent ground-state density profile $n_{\mathrm{TF}}(\mathbf{r})$. The curves shown correspond to a dipole interaction strength $\varepsilon_D = 0.5$ and to various frequency ratios $\omega_x{:}\omega_y{:}\omega_z$ of the harmonic trap: 2:6:3, purple open diamond; 3:6:2, purple solid diamond; 3:2:6, red open square; 6:2:3, red solid square; 1:2:2, blue open circle; 2:2:1, blue solid circle; 2:3:6, green open triangle; 6:3:2, green solid triangle.

For a general triaxial ellipsoid $\mathbb{D}_{\mathrm{TF}}$ the normalization integral

$$\int_{\mathbb{D}_{\mathrm{TF}}} d^3r' n_{\mathrm{TF}}(\mathbf{r}') = N \tag{18}$$

leads to

$$N = \frac{8\pi}{15}\lambda_x\lambda_y\lambda_z n_0. \tag{19}$$

So the problem is to determine from (11) the three semiaxes $\lambda_x$, $\lambda_y$, $\lambda_z$, the orientational angle $\vartheta_0$ and the chemical potential $\mu$.

As has been emphasized by Eberlein *et al.* in Ref. [10] the central task in solving the Thomas-Fermi integral equation (11) is to calculate the potential function

$$\phi_{\mathrm{TF}}(\mathbf{r}) = \frac{1}{4\pi}\int_{\mathbb{D}_{\mathrm{TF}}} d^3r' \frac{1}{|\mathbf{r} - \mathbf{r}'|} n_{\mathrm{TF}}(\mathbf{r}') \tag{20}$$

for a *heterogeneous* particle density distribution $n_{\mathrm{TF}}(\mathbf{r})$. Then, because

$$-\nabla^2\phi_{\mathrm{TF}}(\mathbf{r}) = n_{\mathrm{TF}}(\mathbf{r}), \tag{21}$$

the Thomas-Fermi integral equation (11)

$$(1 - \varepsilon_D)\, n_{\mathrm{TF}}(\mathbf{r}) - 3\varepsilon_D \frac{\partial^2}{\partial r_z^2}\phi_{\mathrm{TF}}(\mathbf{r}) = \frac{\mu - V_T(\mathbf{r})}{g_s} \tag{22}$$

becomes (in free space) equivalent to a partial differential equation of potential theory:

$$-\left[(1 - \varepsilon_D)\left(\frac{\partial^2}{\partial r_x^2} + \frac{\partial^2}{\partial r_y^2}\right) + (1 + 2\varepsilon_D)\frac{\partial^2}{\partial r_z^2}\right]\phi_{\mathrm{TF}}(\mathbf{r}) = \frac{\mu - V_T(\mathbf{r})}{g_s}. \tag{23}$$

In order that the differential operator on the left-hand side is positive definite it is required that

$$-\tfrac{1}{2} < \varepsilon_D < 1. \tag{24}$$

Due to the $d_{z^2}$ anisotropy of the dipole-dipole interaction between two *spin-polarized* atoms at positions $\mathbf{r}$ and $\mathbf{r}'$ the dipole-dipole interaction part of the potential $U(\mathbf{r},\mathbf{r}')$ is attractive *or* repulsive, depending on the orientation of the distance vector $\mathbf{r}-\mathbf{r}'$ relative to the field vector $\mathbf{B}$. So, if $\varepsilon_D > 1$ or $\varepsilon_D < -\frac{1}{2}$, attractive forces prevail and the system will collapse. Of course, a better criterion for stability is to calculate the frequencies of the collective modes of the dipolar interacting BEC. We shall present in the next section results for quadrupolarlike modes of the density fluctuations around the ground-state density profile $n_{\mathrm{TF}}(\mathbf{r})$.

The differential equation (23) makes it manifest that the integral operator with integration domain $\mathbb{D}_{\mathrm{TF}}$ and kernel $\frac{1}{|\mathbf{r}-\mathbf{r}'|}$ in the Thomas-Fermi integral equation (22) for $\mathbf{r} \in \mathbb{D}_{\mathrm{TF}}$ maps a *quadratic* form $n_{\mathrm{TF}}(\mathbf{r})$ spanned by the linearly independent basis functions $\{1,r_a r_b\}_{a\leqslant b\in\{x,y,z\}}$ into a *quartic* form $\phi_{\mathrm{TF}}(\mathbf{r})$ spanned by linearly independent basis functions $\{1,r_a r_b,r_a r_b r_c r_d\}_{a\leqslant b\leqslant c\leqslant d\in\{x,y,z\}}$. Because for a *harmonic* trap potential $V_T(\mathbf{r})$ the right-hand side of (23) is (by definition) a quadratic form, the problem would be exactly solved, provided the coefficients of the quadratic form presented by the derivatives $\frac{\partial^2}{\partial r_a^2}\phi_{\mathrm{TF}}(\mathbf{r})$ of the potential function (20) can be found.

We describe now a very convenient method to determine the coefficients of the quadratic form $\frac{\partial^2}{\partial r_z^2}\phi_{\mathrm{TF}}(\mathbf{r})$, which is all we need to solve the Thomas-Fermi integral equation (22). As a matter of fact, three-dimensional integrals of the type

$$\Phi_l(\mathbf{s}) = \frac{1}{4\pi}\int_{\mathbb{D}} d^3s' \frac{1}{|\mathbf{s}-\mathbf{s}'|}\left(1-\frac{s_x'^2}{\lambda_x^2}-\frac{s_y'^2}{\lambda_y^2}-\frac{s_z'^2}{\lambda_z^2}\right)^l$$
$$l = 0,1,2,3,\ldots, \quad (25)$$
$$\mathbb{D} = \left\{\mathbf{s}'\in\mathbb{R}^3 | \frac{s_x'^2}{\lambda_x^2}+\frac{s_y'^2}{\lambda_y^2}+\frac{s_z'^2}{\lambda_z^2}\leqslant 1\right\}$$

have been calculated analytically by Chandrasekhar [11] in his magisterial treatment of the ellipsoidal figures of equilibrium of gravitating and rotating gas clouds in astrophysics. He showed that $\Phi_l(\mathbf{s})$ can be represented *exactly* in terms of singularity free fast convergent *one-dimensional* integrals. Chandrasekhar's result for the three-dimensional integral $\Phi_l(\mathbf{s})$ at an *internal* point of the ellipsoid $\mathbb{D}$ is

$$\mathbf{s}\in\mathbb{D}_{\mathrm{TF}},$$
$$l = 0,1,2,3,\ldots,$$
$$\Phi_l(\mathbf{s}) = \frac{\lambda_x\lambda_y\lambda_z}{4}\frac{1}{l+1}\int_0^\infty \frac{du}{\sqrt{[(\lambda_x^2+u)(\lambda_y^2+u)(\lambda_z^2+u)]}} \times\left(1-\frac{s_x^2}{\lambda_x^2+u}-\frac{s_y^2}{\lambda_y^2+u}-\frac{s_z^2}{\lambda_z^2+u}\right)^{l+1}. \quad (26)$$

To solve the Thomas-Fermi integral equation we now make use of this result for the special case $l=1$. Because the Cartesian coordinates $\widetilde{r}_b$ of a point presented in the principal axes frame of the Thomas-Fermi ellipsoid $\mathbb{D}_{\mathrm{TF}}$ are connected to the Cartesian coordinates $r_a$ of that same point in the laboratory frame by a rotation,

$$r_b(\vartheta_0) = \widetilde{r}_b = \sum_{a\in\{x,y,z\}} \mathcal{R}_{ba}(\vartheta_0;\mathbf{e}_y) r_a,$$
$$\mathcal{R}_{ba}(\vartheta_0;\mathbf{e}_y) = \begin{bmatrix}\cos(\vartheta_0) & 0 & \sin(\vartheta_0)\\ 0 & 1 & 0\\ -\sin(\vartheta_0) & 0 & \cos(\vartheta_0)\end{bmatrix}_{ba} \quad (27)$$

and taking into account that under such a rotation $\mathcal{R}(\vartheta_0;\mathbf{e}_y)$ we have $|\mathbf{r}-\mathbf{r}'| = |\widetilde{\mathbf{r}}-\widetilde{\mathbf{r}}'|$, we immediately see that the potential function

$$\phi_{\mathrm{TF}}(\mathbf{r}) = n_0\Phi_1[\widetilde{\mathbf{r}}(\mathbf{r})] \quad (28)$$

at a position $\mathbf{r}\in\mathbb{D}_{\mathrm{TF}}$ is a *quartic* form with regard to the linearly independent basis functions $\{1,r_a r_b,r_a r_b r_c r_d\}_{a\leqslant b\leqslant c\leqslant d\in\{x,y,z\}}$. As a second-order derivative of a quartic the function $\frac{\partial^2}{\partial r_z^2}\phi_{\mathrm{TF}}(\mathbf{r})$ is then manifestly a quadratic form, spanned by a linear combination of the basis functions $\{1,\widetilde{r}_x^2,\widetilde{r}_y^2,\widetilde{r}_z^2,\widetilde{r}_x\widetilde{r}_z\}$ or, taking into account (27), it is spanned by a linear combination of the basis functions $\{1,r_x^2,r_y^2,r_z^2,r_x r_z\}$. The transformation from one basis system to the other is accomplished by the orthogonal transformation (27).

The coefficients $c_{ab}$ of the quadratic form

$$\mathbf{r}\in\mathbb{D}_{\mathrm{TF}},$$
$$\frac{\partial^2}{\partial r_z^2}\phi_{\mathrm{TF}}(\mathbf{r}) = \frac{n_0}{2}\left(-c_{00}+c_{xx}r_x^2+c_{yy}r_y^2+c_{zz}r_z^2+c_{xz}r_x r_z\right) \quad (29)$$

depend on the trap orientation angle $\vartheta_0$ and the semiaxes $\lambda_x$, $\lambda_y$, $\lambda_z$ of the ellipsoid $\mathbb{D}_{\mathrm{TF}}$ via the following one-dimensional integrals:

$$a,b\in\{x,y,z\},$$
$$I_a(\lambda_x,\lambda_y,\lambda_z) = \lambda_x\lambda_y\lambda_z\int_0^\infty \frac{du}{\sqrt{(\lambda_x^2+u)(\lambda_y^2+u)(\lambda_z^2+u)}} \times\frac{1}{(\lambda_a^2+u)},$$
$$I_{ab}(\lambda_x,\lambda_y,\lambda_z) = \lambda_x\lambda_y\lambda_z\int_0^\infty \frac{du}{\sqrt{(\lambda_x^2+u)(\lambda_y^2+u)(\lambda_z^2+u)}} \times\frac{1}{(\lambda_a^2+u)(\lambda_b^2+u)}. \quad (30)$$

In Appendix A some of the properties of these so-called *index integrals* are listed. We find

$$c_{00} = \sin^2(\vartheta_0)I_x+\cos^2(\vartheta_0)I_z,$$
$$c_{xx} = \cos^2(\vartheta_0)\sin^2(\vartheta_0)(I_{xx}+I_{zz})+[\cos^4(\vartheta_0)+\sin^4(\vartheta_0)]I_{zx} +2\sin^2(\vartheta_0)\cos^2(\vartheta_0)(I_{xx}-2I_{zx}+I_{zz}),$$
$$c_{yy} = \sin^2(\vartheta_0)I_{xy}+\cos^2(\vartheta_0)I_{zy},$$
$$c_{zz} = 3[\sin^4(\vartheta_0)I_{xx}+\cos^4(\vartheta_0)I_{zz}+2\sin^2(\vartheta_0)\cos^2(\vartheta_0)I_{zx}],$$
$$c_{xz} = 6\sin(\vartheta_0)\cos(\vartheta_0)[\sin^2(\vartheta_0)(I_{xx}-I_{zx}) +\cos^2(\vartheta_0)(I_{zx}-I_{zz})]. \quad (31)$$

It is advantageous to work in the geometry under consideration not with the basis functions $\{1,r_x^2,r_y^2,r_z^2,r_x r_z\}$ but with the basis functions $\{1,\tilde{r}_x^2,\tilde{r}_y^2,\tilde{r}_z^2,\tilde{r}_x\tilde{r}_z\}$ obtained by a rotation of the coordinate system around the axis $\mathbf{e}_y$ by the trap orientation angle $\vartheta_0$ as defined in (27). The exact solution of the Thomas-Fermi integral equation (22) is then obtained by inserting the corresponding explicit expressions for the quadratic form $\frac{\partial^2}{\partial r_z^2}\phi_{\mathrm{TF}}(\mathbf{r})$ and the trap potential $V_T(\mathbf{r})$. From the condition that the prefactors of the linearly independent basis functions $\{1,\tilde{r}_x^2,\tilde{r}_y^2,\tilde{r}_z^2,\tilde{r}_x\tilde{r}_z\}$ in (22) should vanish identically, the following set of coupled self-consistency equations is found:

$$\left\{1-\varepsilon_D+\frac{3}{2}\varepsilon_D[\sin^2(\vartheta_0)I_x+\cos^2(\vartheta_0)I_z]\right\}n_0=\frac{\mu}{g_s}, \tag{32}$$

$$\left\{\frac{1-\varepsilon_D}{\lambda_x^2}+\frac{3\varepsilon_D}{2}[\cos^2(\vartheta_0)I_{zx}+3\sin^2(\vartheta_0)I_{xx}]\right\}n_0 = \frac{m^\star}{2g_s}\left[\omega_x^2\cos^2(\vartheta_T-\vartheta_0)+\omega_z^2\sin^2(\vartheta_T-\vartheta_0)\right], \tag{33}$$

$$\left\{\frac{1-\varepsilon_D}{\lambda_y^2}+\frac{3\varepsilon_D}{2}[\cos^2(\vartheta_0)I_{zy}+\sin^2(\vartheta_0)I_{xy}]\right\}n_0=\frac{m^\star}{2g_s}\omega_y^2, \tag{34}$$

$$\left\{\frac{1-\varepsilon_D}{\lambda_z^2}+\frac{3\varepsilon_D}{2}[3\cos^2(\vartheta_0)I_{zz}+\sin^2(\vartheta_0)I_{xz}]\right\}n_0 = \frac{m^\star}{2g_s}\left[\omega_x^2\sin^2(\vartheta_T-\vartheta_0)+\omega_z^2\cos^2(\vartheta_T-\vartheta_0)\right], \tag{35}$$

$$\frac{3\varepsilon_D}{2}\sin(2\vartheta_0)I_{xz}n_0=\frac{m^\star}{2g_s}\frac{\omega_x^2-\omega_z^2}{2}\sin(2\vartheta_T-2\vartheta_0). \tag{36}$$

The normalization condition connects the density $n_0$ at the center of the Thomas-Fermi domain $\mathbb{D}_{\mathrm{TF}}$ to the product of the semiaxes:

$$n_0=\frac{15}{8\pi}\frac{N}{\lambda_x\lambda_y\lambda_z}. \tag{37}$$

Let us first write the self-consistency equations without dipole interaction setting $\varepsilon_D=0$. There follows

$$n_0^{(0)}=\frac{\mu^{(0)}}{g_s},\qquad \frac{1}{[\lambda_a^{(0)}]^2}=\frac{m^\star}{2\mu^{(0)}}\omega_a^2. \tag{38}$$

Using the normalization

$$n_0^{(0)}=\frac{15}{8\pi}\frac{N}{\lambda_x^{(0)}\lambda_y^{(0)}\lambda_z^{(0)}} \tag{39}$$

and introducing the definitions

$$\omega=(\omega_x\omega_y\omega_z)^{\frac{1}{3}},\qquad a_\omega=\left(\frac{\hbar}{m^\star\omega}\right)^{\frac{1}{2}}, \tag{40}$$

we obtain for the chemical potential $\mu^{(0)}$ and the semiaxes $\lambda_a^{(0)}$ of a BEC inside an anisotropic harmonic trap in the Thomas-Fermi regime well-known results:

$$\mu^{(0)}(N)=\left(\frac{15}{4\pi}\frac{4\pi Na_s}{a_\omega}\right)^{\frac{2}{5}}\frac{\hbar\omega}{2}, \tag{41}$$

$$\lambda_a^{(0)}(N)=\left(\frac{2\mu^{(0)}}{m^\star\omega_a^2}\right)^{\frac{1}{2}}=\frac{\omega}{\omega_a}\Lambda,\qquad \Lambda=a_\omega\left(\frac{15}{4\pi}\frac{4\pi Na_s}{a_\omega}\right)^{\frac{1}{5}}. \tag{42}$$

The exponent $\frac{2}{5}$ is characteristic for the large $N$ scaling of the chemical potential $\mu^{(0)}(N)$ of a BEC confined inside a *harmonic* trap [1].

The ensuing calculations simplify making use of elementary scaling relations that hold for single- and double-index integrals:

$$I_a(\lambda_x,\lambda_y,\lambda_z)=I_a\left(\frac{\lambda_x}{\lambda_z},\frac{\lambda_y}{\lambda_z},1\right)\equiv\overline{I}_a,\qquad \lambda_c^2I_{ab}(\lambda_x,\lambda_y,\lambda_z)=\frac{\lambda_c^2}{\lambda_z^2}I_{ab}\left(\frac{\lambda_x}{\lambda_z},\frac{\lambda_y}{\lambda_z},1\right)\equiv\frac{\lambda_c^2}{\lambda_z^2}\overline{I}_{ab}. \tag{43}$$

Using the obvious relation

$$\frac{n_0}{n_0^{(0)}}=\frac{\lambda_x^{(0)}\lambda_y^{(0)}\lambda_z^{(0)}}{\lambda_x\lambda_y\lambda_z}, \tag{44}$$

the self-consistency problem posed by (32)–(36) may then be reduced to three coupled equations for the ratios $\frac{\lambda_x}{\lambda_z},\frac{\lambda_y}{\lambda_z}$ and the equilibrium orientation angle $\vartheta_0$ as functions of the trap orientation angle $\vartheta_T$, the trap frequencies $\omega_a$, and the dipole interaction strength parameter $\varepsilon_D$:

$$\frac{\lambda_x^2}{\lambda_z^2}=\frac{\omega_x^2\sin^2(\vartheta_T-\vartheta_0)+\omega_z^2\cos^2(\vartheta_T-\vartheta_0)}{\omega_x^2\cos^2(\vartheta_T-\vartheta_0)+\omega_z^2\sin^2(\vartheta_T-\vartheta_0)}\times\frac{1-\varepsilon_D+\frac{3\varepsilon_D}{2}\frac{\lambda_x^2}{\lambda_z^2}[\cos^2(\vartheta_0)\overline{I}_{zx}+3\sin^2(\vartheta_0)\overline{I}_{xx}]}{1-\varepsilon_D+\frac{3\varepsilon_D}{2}[3\cos^2(\vartheta_0)\overline{I}_{zz}+\sin^2(\vartheta_0)\overline{I}_{xz}]}, \tag{45}$$

$$\frac{\lambda_y^2}{\lambda_z^2}=\frac{\omega_x^2\sin^2(\vartheta_T-\vartheta_0)+\omega_z^2\cos^2(\vartheta_T-\vartheta_0)}{\omega_y^2}\times\frac{1-\varepsilon_D+\frac{3\varepsilon_D}{2}\frac{\lambda_y^2}{\lambda_z^2}[\cos^2(\vartheta_0)\overline{I}_{yz}+\sin^2(\vartheta_0)\overline{I}_{xy}]}{1-\varepsilon_D+\frac{3\varepsilon_D}{2}[3\cos^2(\vartheta_0)\overline{I}_{zz}+\sin^2(\vartheta_0)\overline{I}_{xz}]}, \tag{46}$$

$$\tan(2\vartheta_0)=\frac{\left(\omega_x^2-\omega_z^2\right)\sin\left(2\vartheta_T\right)}{\left(\omega_x^2-\omega_z^2\right)\cos\left(2\vartheta_T\right)+3\varepsilon_D\frac{\lambda_y^2}{\lambda_z^2}\overline{I}_{xz}\frac{\omega_y^2}{1-\varepsilon_D+\frac{3\varepsilon_D}{2}\frac{\lambda_y^2}{\lambda_z^2}[\cos^2(\vartheta_0)\overline{I}_{zy}+\sin^2(\vartheta_0)\overline{I}_{xy}]}}. \tag{47}$$

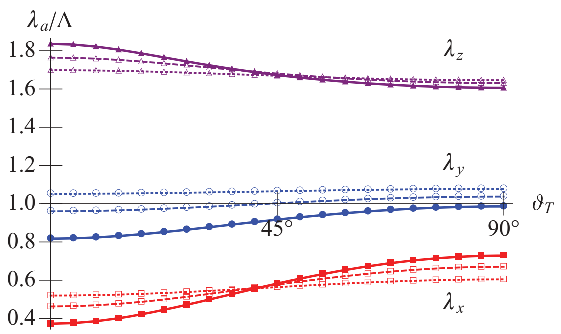


FIG. 3. (Color online) Plot of semiaxes $\lambda_x$, $\lambda_y$, and $\lambda_z$ of self-consistent ground-state density profile $n_{\mathrm{TF}}(\mathbf{r})$ vs trap orientation angle $\vartheta_T$ for various dipolar interaction strength $\varepsilon_D$:$\varepsilon_D = 0.2$, dotted line; $\varepsilon_D = 0.5$, dashed line; $\varepsilon_D = 0.8$, solid line. The ratio of trap frequencies is $\omega_x$:$\omega_y$:$\omega_z$ = 6:3:2.

We have found that the set of self-consistency equations (45), (46), and (47) may be conveniently solved numerically by the method of fixed point iteration. Using identities like

$$\cos^2(\vartheta_0) = \frac{1}{2} + \frac{1}{2}\frac{1}{\sqrt{1+\tan^2(2\vartheta_0)}}$$

the evaluation of trigonometric functions in the iteration process can be completely avoided.

Once the ratios $\frac{\lambda_x}{\lambda_z}, \frac{\lambda_y}{\lambda_z}$ and the orientation angle $\vartheta_0$ are known, it follows directly from (35) and (59) that

$$\lambda_z = \left[\frac{\frac{\omega_z^2}{\omega_x\omega_y}}{\frac{\lambda_x}{\lambda_z}\frac{\lambda_y}{\lambda_z}} \frac{1-\varepsilon_D+\frac{3\varepsilon_D}{2}[3\cos^2(\vartheta_0)\overline{I}_{zz}+\sin^2(\vartheta_0)\overline{I}_{xz}]}{\frac{\omega_x^2}{\omega_z^2}\sin^2(\vartheta_T-\vartheta_0)+\cos^2(\vartheta_T-\vartheta_0)}\right]^{\frac{1}{5}}\lambda_z^{(0)},$$

$$\lambda_x = \frac{\lambda_x}{\lambda_z}\lambda_z, \quad \lambda_y = \frac{\lambda_y}{\lambda_z}\lambda_z. \qquad (48)$$

For the special case of an *isotropic* harmonic trap [1] the principal effect of the dipole-dipole interaction on the ground-state density profile $n_{\mathrm{TF}}(\mathbf{r})$ of a dipolar interacting BEC is the well-known elongation of the semiaxis $\lambda_z$ parallel to $\mathbf{B}$, and the distortion of the semiaxes $\lambda_x = \lambda_y$ perpendicular to $\mathbf{B}$ toward smaller values:

$$\frac{\lambda_x}{\lambda_z} = \frac{1-\frac{1}{5}\varepsilon_D+\cdots}{1+\frac{2}{5}\varepsilon_D+\cdots}. \qquad (49)$$

In Figs. 2 and 3 self-consistent solutions of the coupled equations (45), (46), and (47) for the equilibrium angle $\vartheta_0 - \vartheta_T$ and the semiaxes $\lambda_a$ are plotted as functions of the trap orientation angle $\vartheta_T$ for various magnetic dipole interaction strength parameters $\varepsilon_D$, assuming a triaxial trap anisotropy ratio $\omega_x$:$\omega_y$:$\omega_z$ = 6:3:2.

Once the semiaxes $\lambda_a$ of the particle density $n_{\mathrm{TF}}(\mathbf{r})$ (15) are determined, then (44) gives us the value $n_0$ of the density of the ellipsoidal shaped BEC at its center. In Fig. 4 the ratio $\frac{n_0}{n_0^{(0)}}$ is plotted vs the trap orientation angle $\vartheta_T$, the inset showing for selected trap orientation angles $\vartheta_T \in \{0, \frac{\pi}{4}, \frac{\pi}{2}\}$ cuts of the corresponding self-consistently determined Thomas-Fermi ellipsoid $\mathbb{D}_{\mathrm{TF}}$ with the symmetry plane $y = 0$. For a prolate trap the density is largest for $\vartheta_T = 0$, because the net mutual dipole force between atom pairs inside the domain $\mathbb{D}_{\mathrm{TF}}$ is attractive. As $\vartheta_T$ increases the density $n_0$ becomes smaller and assumes

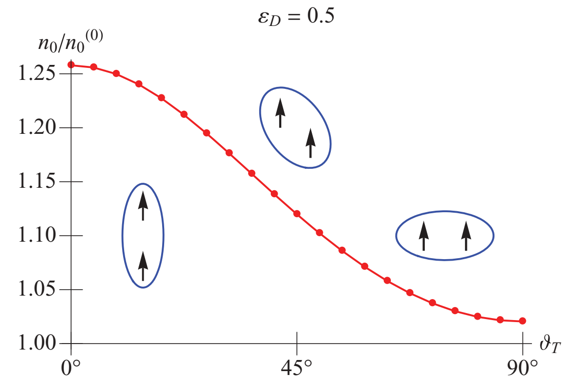


FIG. 4. (Color online) Self-consistent particle density $n_0$ at the center position of the anisotropic harmonic trap plotted vs trap orientation angle $\vartheta_T$. The inset displays cuts of the Thomas-Fermi ellipsoid $\mathbb{D}_{\mathrm{TF}}$ with the symmetry plane $y = 0$ for trap orientation angles $\vartheta_T = 0°$, $\vartheta_T = 45°$, and $\vartheta_T = 90°$. The ratio of trap frequencies is $\omega_x$:$\omega_y$:$\omega_z$ = 2:2:1, and the dipole interaction strength is $\varepsilon_D = 0.5$.

a minimum at $\vartheta_T = 90°$, because for a parallel alignment the net mutual dipole force between atom pairs inside the domain $\mathbb{D}_{\mathrm{TF}}$ is repulsive.

Finally, there follows from (32) an explicit formula for the chemical potential:

$$\mu = \left\{1-\varepsilon_D+\frac{3}{2}\varepsilon_D[\sin^2(\vartheta_0)\overline{I}_x+\cos^2(\vartheta_0)\overline{I}_z]\right\}\frac{n_0}{n_0^{(0)}}\mu^{(0)}(N). \qquad (50)$$

The dependence of $\mu$ on particle number $N$ is solely described by the factor $\mu^{(0)}(N)$, i.e., the ratio $\frac{\mu}{\mu^{(0)}}$ is independent of particle number $N$. In Fig. 5 the chemical potential $\mu$ is plotted vs the trap orientation angle $\vartheta_T$ for different values of the dipole interaction strength $\varepsilon_D$. While for an *isotropic* harmonic trap the chemical potential $\mu$ does not change to first order in $\varepsilon_D$, one finds for an *anisotropic* harmonic trap, making a straightforward expansion to the first order in the dipole interaction strength $\varepsilon_D$, for the case of an oblate (pancake shaped) trap that $[\frac{d\mu}{d\varepsilon_D}]_{\varepsilon_D=0} > 0$ and for a prolate (cigar shaped) trap that $[\frac{d\mu}{d\varepsilon_D}]_{\varepsilon_D=0} < 0$, respectively.

The displayed characteristic dependence of chemical potential $\mu$ on the trap orientation angle $\vartheta_T$ should be observable

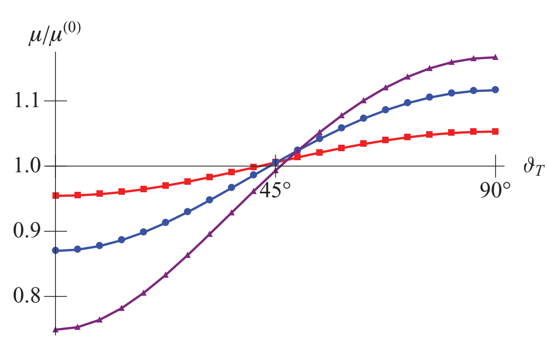


FIG. 5. (Color online) Chemical potential $\mu$ vs trap orientation angle $\vartheta_T$ for different values of dipole interaction strength. $\varepsilon_D = 0.2$, red square; $\varepsilon_D = 0.5$, blue circle; $\varepsilon_D = 0.8$, purple triangle. The ratio of trap frequencies is $\omega_x$:$\omega_y$:$\omega_z$ = 6:3:2.

as the release energy $E_r$ of a spin-polarized dipolar interacting BEC confined in a harmonic trap, when the trap potential is suddenly switched off to zero, and subsequently the dilute atom gas cloud undergoes a *ballistic* expansion [3]. We find within the range of validity of the Thomas-Fermi approximation that there holds also in the presence of long-ranged dipole-dipole interactions

$$E_r = E_{\text{int}} = \tfrac{2}{7}\mu N. \tag{51}$$

As a matter of fact, the total energy

$$E = \langle \widehat{H} \rangle_\Psi = \langle \widehat{H}_{\text{kin}} + \widehat{H}_{\text{pot}} + \widehat{H}_{\text{int}} \rangle_\Psi \tag{52}$$

and the interaction energy $E_{\text{int}} = \langle \widehat{H}_{\text{int}} \rangle_\Psi$ are connected in the ground state $\Psi$ of the BEC, see (1), by the general relation

$$E = \mu N - E_{\text{int}}. \tag{53}$$

This applies because the *optimal* one-particle wave function $\psi(\mathbf{r})$ building the $N$ particle ground state $\Psi$ solves the Gross-Pitaevskii (GP) equation, so the expectation value $\langle \widehat{H}_{\text{kin}} \rangle_\Psi$of the kinetic energy can be reexpressed via the GP equation in terms of the chemical potential $\mu$ and the interaction energy $E_{\text{int}}$. On the other hand, the total energy $E$ of the BEC is connected to the chemical potential $\mu$ by the general relation

$$\mu = \frac{\partial E}{\partial N}. \tag{54}$$

It follows from (50), and the established scaling (41) of $\mu^{(0)}(N) \propto N^{\frac{2}{5}}$ for a large particle number $N \gg 1$, that up to a constant that is independent of $N$ there also holds for a spin-polarized dipolar BEC confined inside a *harmonic* trap the well-known relation [1]

$$E = \tfrac{5}{7}\mu N \tag{55}$$

and therefore

$$E_{\text{int}} = \mu N - E = \tfrac{2}{7}\mu N. \tag{56}$$

## III. COLLECTIVE MODES OF SMALL-AMPLITUDE DENSITY OSCILLATIONS

### A. Parametrization of low-lying excitations in triaxial harmonic trap

An important test of the macroscopic quantum physics of a BEC is the study of elementary excitations above the ground state. One technique to excite low-energy collective modes of a BEC is to suddenly modify the trap potential. For example, shifting the center of the trap excites the dipole modes, that is, the motion of the center of mass of a BEC cloud around its equilibrium position in a harmonic trap. Changing the curvature of the trap by switching the trap frequencies may excite the breather mode. In an anisotropic harmonic trap there also exist the so-called scissors modes [12], which can be excited by rotating a principal axis of the trap, thus pushing the atom cloud in the trap away from equilibrium. A recently reported elegant new experimental technique excites a BEC by modulating the field dependence of the atomic scattering length $a_s$ near to a magnetic Feshbach resonance [13–15].

In this section we calculate for the case of a harmonic anisotropic trap with arbitrary trap orientation angle $\vartheta_T$ the small-amplitude collective modes of a dipolar interacting spin-polarized BEC at very low energy, so the wavelength of the excitations becomes comparable to the size of the Thomas-Fermi length $\Lambda$. For a large number $N \gg 1$ of particles in the BEC the particle density $n(\mathbf{r},t)$ and the macroscopic Josephson phase $S(\mathbf{r},t)$ are *conjugate* variables, so the collective dynamics of the system (ignoring a small quantum pressure) is governed by the standard canonical equations of motion of macroscopic quantum physics [1]:

$$\hbar \frac{\partial}{\partial t} S(\mathbf{r},t) = -\frac{\hbar^2}{2m^\star} \sum_{a\in\{x,y,z\}} \left(\frac{\partial S(\mathbf{r},t)}{\partial r_a}\right)^2 - V_T(\mathbf{r}) - \int_{\mathbb{D}(t)} d^3r'\, U(\mathbf{r},\mathbf{r}')\, n(\mathbf{r}',t), \tag{57}$$

$$\frac{\partial}{\partial t} n(\mathbf{r},t) + \frac{\hbar}{m^\star} \sum_{a\in\{x,y,z\}} \frac{\partial}{\partial r_a}\left[n(\mathbf{r},t)\frac{\partial S(\mathbf{r},t)}{\partial r_a}\right] = 0. \tag{58}$$

The gradient of the phase, the velocity field $\mathbf{v}(\mathbf{r},t) = \frac{\hbar}{m^\star}\nabla \delta s(\mathbf{r},t)$, is directly connected to the density of the particle current, $\mathbf{j}(\mathbf{r},\mathbf{t}) = n(\mathbf{r},t)\mathbf{v}(\mathbf{r},t)$ [1]. The quasiclassical Josephson equation (57) and the continuity equation (58) need to be solved subject to the normalization condition

$$\int_{\mathbb{D}(t)} d^3r\; n(\mathbf{r},t) = N, \tag{59}$$

where for a fluctuating particle density $n(\mathbf{r},t)$ the positivity domain

$$\mathbb{D}(t) = \{\mathbf{r} \in \mathbb{R}^3 |\; n(\mathbf{r},t) > 0\} \tag{60}$$

depends (in principle) on time too.

Let us assume a perturbation expansion of phase and density of the form

$$\begin{aligned} S(\mathbf{r},t) &= -\frac{\mu}{\hbar}t + \delta s\,(\mathbf{r},t), \\ n(\mathbf{r},t) &= n_{\text{TF}}(\mathbf{r}) + \delta n\,(\mathbf{r},t), \end{aligned} \tag{61}$$

with $\delta s\,(\mathbf{r},t)$ and $\delta n\,(\mathbf{r},t)$ denoting small fluctuations of phase and particle density around the ground state of the BEC.

For convenience we work from now on, unless otherwise explicitly stated, in the principal axes frame of the Thomas-Fermi ellipsoid $\mathbb{D}_{\text{TF}}$. As is indicated in Fig. 1, for a trap orientation angle $\vartheta_T \neq 0$, the magnetic field $\mathbf{B}$ is not aligned parallel to the principal axis vector $\mathbf{e}_{z,0}$ of the ellipsoid $\mathbb{D}_{\text{TF}}$. In this case the interaction energy $U(\mathbf{r},\mathbf{r}')$ between two spin-polarized atoms at position $\mathbf{r}$ and $\mathbf{r}'$, both carrying a magnetic dipole moment $\langle \mathbf{M} \rangle = (2\mu_B S)\,\mathbf{m}$ orientated (anti)parallel to $\mathbf{B}$, is then given by

$$U(\mathbf{r},\mathbf{r}') = g_s\left[(1-\varepsilon_D)\delta^{(3)}(\mathbf{r}-\mathbf{r}') - 3\varepsilon_D(\mathbf{m}\cdot\nabla_{\mathbf{r}})^2\frac{1}{4\pi}\frac{1}{|\mathbf{r}-\mathbf{r}'|}\right]. \tag{62}$$

In the geometry under consideration the axis $\mathbf{e}_{z,0}$ of the ellipsoid $\mathbb{D}_{\text{TF}}$ is rotated around the axis $\mathbf{e}_{y,T}$ of the trap by an angle $\vartheta_0$, and we assume $\mathbf{m} \perp \mathbf{e}_y$:

$$(\mathbf{m}\cdot\nabla_{\mathbf{r}})^2 = \sin^2(\vartheta_0)\frac{\partial^2}{\partial r_x^2} + \cos^2(\vartheta_0)\frac{\partial^2}{\partial r_z^2} + \sin(2\vartheta_0)\frac{\partial^2}{\partial r_x \partial r_z}. \tag{63}$$

Upon linearization of (57) and (58), in the expansion we reproduce the Thomas-Fermi integral equation (11) to zero order, determining the equilibrium density profile $n_{\mathrm{TF}}(\mathbf{r})$ and the chemical potential $\mu$, as discussed in the previous section.

To derive the equations of motion for the fluctuations of the phase $\delta s(\mathbf{r},t)$ and the density $\delta n(\mathbf{r},t)$, let us first consider for a kernel $K(\mathbf{r},\mathbf{r}')$ that couples to particle density $n(\mathbf{r}',t)$ the associated fluctuation

$$\delta K(t) = \int_{\mathbb{D}(t)} d^3r' K(\mathbf{r},\mathbf{r}')\, n(\mathbf{r}',t) - \int_{\mathbb{D}_{\mathrm{TF}}} d^3r' K(\mathbf{r},\mathbf{r}')\, n_{\mathrm{TF}}(\mathbf{r}'). \tag{64}$$

In principle there are two contributions to $\delta K(t)$. One is generated by the time dependence of the density distribution, and the other results from a change of the integration domain $\mathbb{D}(t)$. Introducing the Heaviside distribution

$$\Theta_H(x) = \frac{1+\mathrm{sgn}(x)}{2}, \tag{65}$$

we rewrite (64) as

$$\delta K(t) = \int d^3r' K(\mathbf{r},\mathbf{r}')\{\Theta_H[n_{\mathrm{TF}}(\mathbf{r}') + \delta n(\mathbf{r}',t)] \times [n_{\mathrm{TF}}(\mathbf{r}') + \delta n(\mathbf{r}',t)] - \Theta_H[n_{\mathrm{TF}}(\mathbf{r}')] n_{\mathrm{TF}}(\mathbf{r}')\}. \tag{66}$$

An expansion to the first order in the small quantitiy $\delta n$ leads to

$$\delta K(t) = \int d^3r' K(\mathbf{r},\mathbf{r}')\delta n(\mathbf{r}',t)\{\Theta[n_{\mathrm{TF}}(\mathbf{r}')] + n_{\mathrm{TF}}(\mathbf{r}')\delta_D[n_{\mathrm{TF}}(\mathbf{r}')]\} + o(|\delta n|^2), \tag{67}$$

where $\delta_D(x)$ denotes the Dirac-delta distribution:

$$\delta_D(x) = \frac{d}{dx}\Theta_H(x). \tag{68}$$

Here, the term proportional to $n_{\mathrm{TF}}(\mathbf{r}')\,\delta_D[n_{\mathrm{TF}}(\mathbf{r}')]$ corresponds to a surface integral over the boundary $\partial\mathbb{D}_{\mathrm{TF}}$ of the Thomas-Fermi domain $\mathbb{D}_{\mathrm{TF}}$. However, because $n_{\mathrm{TF}}(\mathbf{r}') \equiv 0$ for $\mathbf{r}' \in \partial\mathbb{D}_{\mathrm{TF}}$ the value of this surface integral is zero. This means the fluctuation of the integration domain $\mathbb{D}(t)$ around the shape of the *equilibrium* cloud $\mathbb{D}_{\mathrm{TF}}$ as caused by a density fluctuation $\delta n = n(\mathbf{r},t) - n_{\mathrm{TF}}(\mathbf{r})$ represents only a small correction to $\delta K(t)$ beyond first-order accuracy:

$$\delta K(t) = \int_{\mathbb{D}_{\mathrm{TF}}} d^3r' K(\mathbf{r},\mathbf{r}')\,\delta n(\mathbf{r}',t) + o(|\delta n|^2). \tag{69}$$

It follows now directly from (57) for the time derivative of the phase fluctuation $\delta s(\mathbf{r},t)$, substituting the special case $K(\mathbf{r},\mathbf{r}') = U(\mathbf{r},\mathbf{r}')$ into (69), that

$$\hbar\frac{\partial}{\partial t}\delta s(\mathbf{r},t) = -\int_{\mathbb{D}_{\mathrm{TF}}} d^3r' U(\mathbf{r},\mathbf{r}')\delta n(\mathbf{r}',t) \tag{70}$$

and, further, from (58),

$$a \in \{x,y,z\},\quad 0 = \frac{\partial^2}{\partial t^2}\delta n(\mathbf{r},t) + \frac{1}{m^\star}\sum_a \frac{\partial}{\partial r_a}\left[n_{\mathrm{TF}}(\mathbf{r})\frac{\partial}{\partial r_a}\hbar\frac{\partial}{\partial t}\delta s(\mathbf{r},t)\right]. \tag{71}$$

This is the well-known wave equation describing the collective density excitations of a BEC in the quantum hydrodynamic limit [1] for the case of a nonlocal interaction potential $U(\mathbf{r},\mathbf{r}')$.

In the ensuing discussion we consider the collective modes of small-amplitude oscillations around the equilibrium density distribution $n_{\mathrm{TF}}(\mathbf{r})$ in the trap. The corresponding density fluctuations $\delta n(\mathbf{r},t)$ may be expanded with respect to a set of linearly independent multinomials $\{1,r_a,r_ar_b,r_ar_br_c,\ldots\}_{a\leqslant b\leqslant c\cdots}$:

$$a,b,c \in \{x,y,z\},\quad \delta n(\mathbf{r},t) = \delta n^{(0)}(t) + \sum_a \delta n_a^{(1)}(t)\, r_a + \sum_{a,b}\delta n_{ab}^{(2)}(t) r_a r_b + \sum_{a,b,c}\delta n_{abc}^{(3)}(t) r_a r_b r_c \cdots. \tag{72}$$

We restrict here to the terms of zero order, first order, and second order of the density fluctuation $\delta n(\mathbf{r},t)$ as described by amplitudes $\delta n^{(0)}(t)$, $\delta n_a^{(1)}(t)$, and $\delta n_{ab}^{(2)}(t)$, respectively. Third- and higher-order terms proportional to $\delta n_{abc}^{(3)}(t)$, etc., are considered elsewhere [16].

A very convenient approach to the determination of the small-amplitude oscillations $\delta n(\mathbf{r},t)$ around the equilibrium density $n_{\mathrm{TF}}(\mathbf{r}) \equiv n_{\mathrm{TF}}(\mathbf{r};\boldsymbol{\lambda})$ is to parametrize the density fluctuations $\delta n(\mathbf{r},t)$ in terms of a *displacement* vector field $\boldsymbol{\eta}(\mathbf{r},t)$ and in terms of a *dilatation* amplitude vector $\boldsymbol{\zeta}(t)$:

$$\delta n(\mathbf{r},t) = n_{\mathrm{TF}}[\mathbf{r} + \boldsymbol{\eta}(\mathbf{r},t); \boldsymbol{\lambda} + \boldsymbol{\zeta}(t)] - n_{\mathrm{TF}}(\mathbf{r};\boldsymbol{\lambda}). \tag{73}$$

Neglecting small higher-order terms regarding the size of the amplitudes $|\boldsymbol{\eta}|$ and $|\boldsymbol{\zeta}|$, a general density fluctuation $\delta n(\mathbf{r},t)$ around the ground state of the BEC cloud is then

$$b \in \{x,y,z\},\quad \delta n(\mathbf{r},t) = \sum_b\left[\frac{\partial n_{\mathrm{TF}}(\mathbf{r};\boldsymbol{\lambda})}{\partial r_b}\eta_b(\mathbf{r},t) + \frac{\partial n_{\mathrm{TF}}(\mathbf{r};\boldsymbol{\lambda})}{\partial \lambda_b}\zeta_b(t)\right] + o(|\boldsymbol{\eta}|^2 + |\boldsymbol{\zeta}|^2). \tag{74}$$

It follows directly from atom number conservation, and substituting the special case $K(\mathbf{r},\mathbf{r}') \equiv 1$ into (69), that

$$\int_{\mathbb{D}_{\mathrm{TF}}} d^3r'\delta n(\mathbf{r}',t) = 0. \tag{75}$$

Upon insertion of (74) into (75), and using the theorem of Gauß, we see that the displacement vector field $\boldsymbol{\eta}(\mathbf{r},t)$ is necessarily a *solenoidal* vector field:

$$\mathrm{div}\boldsymbol{\eta}(\mathbf{r},t) = 0. \tag{76}$$

Making a partial integration this property of $\boldsymbol{\eta}(\mathbf{r},t)$ implies for the phase fluctuation (70)

$$b \in \{x,y,z\},$$
$$\hbar\frac{\partial}{\partial t}\delta s(\mathbf{r},t) = \sum_b \left[ \int_{\mathbb{D}_{\rm TF}} d^3r'\eta_b(\mathbf{r}',t)\frac{\partial U(\mathbf{r},\mathbf{r}')}{\partial r'_b} n_{\rm TF}(\mathbf{r}';\boldsymbol{\lambda}) - \zeta_b(t)\frac{\partial}{\partial\lambda_b}\int_{\mathbb{D}_{\rm TF}} d^3r' U(\mathbf{r},\mathbf{r}')\, n_{\rm TF}(\mathbf{r}';\boldsymbol{\lambda})\right]. \tag{77}$$

A simplification results for the standard two-body interaction forces among two atoms, say at positions $\mathbf{r}$ and $\mathbf{r}'$, that obey Newton's law "actio = reactio":

$$\frac{\partial U(\mathbf{r},\mathbf{r}')}{\partial r'_b} = -\frac{\partial U(\mathbf{r},\mathbf{r}')}{\partial r_b}. \tag{78}$$

Then a general density fluctuation $\delta n(\mathbf{r},t)$ around equilibrium, as parametrized by (74) in terms of a solenoidal displacement $\boldsymbol{\eta}(\mathbf{r},t)$ and a *dilatation* amplitude $\boldsymbol{\zeta}(t)$, is connected to the time derivative of the fluctuation $\delta s(\mathbf{r},t)$ of the Josephson phase by

$$b \in \{x,y,z\},$$
$$\hbar\frac{\partial}{\partial t}\delta s(\mathbf{r},t) = -\sum_b \left[\frac{\partial}{\partial r_b}\int_{\mathbb{D}_{\rm TF}} d^3r' U(\mathbf{r},\mathbf{r}')n_{\rm TF}(\mathbf{r}';\boldsymbol{\lambda})\eta_b(\mathbf{r}',t) + \zeta_b(t)\frac{\partial}{\partial\lambda_b}\int_{\mathbb{D}_{\rm TF}} d^3r' U(\mathbf{r},\mathbf{r}')\, n_{\rm TF}(\mathbf{r}';\boldsymbol{\lambda})\right]. \tag{79}$$

Indeed, this exact representation of the quasiclassical hydrodynamic phase fluctuations of a BEC for interactions $U(\mathbf{r},\mathbf{r}')$ that obey (78) represents a convenient starting point for our analytic calculation of the collective density oscillations of a spin-polarized dipolar interacting BEC in a trap.

Like the density fluctuations in (72) we may also expand the Cartesian components $\eta_a(\mathbf{r},t)$ of the displacement vector field:

$$a,b,c \in \{x,y,z\},$$
$$\eta_a(\mathbf{r},t) = \eta_a^{(0)}(t) + \sum_b \eta_{ab}^{(1)}(t)\, r_b + \sum_{b,c}\eta_{abc}^{(2)}(t)\, r_b r_c \cdots. \tag{80}$$

The zero-order term $\eta_a^{(0)}(t)$ describes a *homogeneous* displacement of the center of mass of a BEC cloud in a trap. Actually, any system of particles that interact via two-body forces obeying (78) has the property that the motion of the center of mass separates from the equations of motion of the other degrees of freedom of the system. As a result, the frequency of the dipole modes of a trapped atom gas cloud is independent of any such interactions, because the center of mass of the cloud moves like a single particle of mass $Nm^\star$ in the external trap potential $V_T(\mathbf{r})$. For a harmonic trap, the frequencies of the dipole modes coincide, therefore, with the bare frequencies $\omega_a$ of the trap. In experiments this feature is useful to measure and calibrate the trap frequencies.

The first-order terms $\eta_{ab}^{(1)}(t)$ together with the displacement amplitudes $\zeta_b(t)$ are connected to density oscillations with $s$-wave and $d$-wave symmetry. Second-order displacement amplitudes like $\eta_{abc}^{(2)}(t)$ are connected to the octupolar collective density excitations $\delta n_{abc}^{(3)}(t)$. These and even higher-order modes are considered elsewhere [16].

It follows directly from (74) that only certain linear combinations of the first-order displacement amplitudes $\eta_{ab}^{(1)}(t)$ together with the dilatation amplitudes $\zeta_b(t)$ couple to $s$-wave and $d$-wave symmetry density oscillation amplitudes $\delta n^{(0)}(t)$ and $\delta n_{ab}^{(2)}(t)$, while the homogeneous zero-order displacement amplitudes $\eta_a^{(0)}(t)$ couple to the dipole modes:

$$\delta n(\mathbf{r},t) = 2n_0\Bigg[\frac{1}{\lambda_x^2}\rho_{xx}(t)r_x^2 + \frac{1}{\lambda_y^2}\rho_{yy}(t)r_y^2 + \frac{1}{\lambda_z^2}\rho_{zz}(t)r_z^2 - \frac{1}{2}\left(1 - \frac{r_x^2}{\lambda_x^2} - \frac{r_y^2}{\lambda_y^2} - \frac{r_z^2}{\lambda_z^2}\right)\rho_{00}(t) + \sum_{a<b}\frac{1}{\lambda_a\lambda_b}\rho_{ab}(t)r_a r_b + \frac{1}{\lambda_x^2}\rho_x(t)r_x + \frac{1}{\lambda_y^2}\rho_y(t)r_y + \frac{1}{\lambda_z^2}\rho_z(t)r_z\Bigg], \tag{81}$$

where

$$a,b \in \{x,y,z\},$$
$$\rho_{ab}(t) = \delta_{ab}\left[\frac{\zeta_a(t)}{\lambda_a} - \eta_{aa}^{(1)}(t)\right] - (1-\delta_{ab})\lambda_a\lambda_b\left[\frac{1}{\lambda_a^2}\eta_{ab}^{(1)}(t) + \frac{1}{\lambda_b^2}\eta_{ba}^{(1)}(t)\right],$$
$$\rho_{00}(t) = \sum_a \rho_{aa}(t),$$
$$\rho_a(t) = -\eta_a^{(0)}(t). \tag{82}$$

Particle number conservation implies the solenoidal constraint

$$\eta_{xx}^{(1)}(t) + \eta_{yy}^{(1)}(t) + \eta_{zz}^{(1)}(t) = 0 \tag{83}$$

so there follows immediately

$$\rho_{00}(t) = \sum_a \rho_{aa}(t) = \frac{\zeta_x(t)}{\lambda_x} + \frac{\zeta_y(t)}{\lambda_y} + \frac{\zeta_z(t)}{\lambda_z}. \tag{84}$$

In general, a BEC cloud may get excited by a combination of actions, involving translations of the trap minimum, rotations of the trap axes, or changes of the curvature of the trap. The homogeneous displacement amplitudes $\eta_a^{(0)}(t)$ correspond to infinitesimal translations of the position of the center of the BEC cloud. Thus, a density oscillation with a dipolar $p$-wave symmetry proportional to $\rho_a(t)$ can be excited by a translation of the minimum of the trap. Being mainly interested in the effect of interactions on the collective modes, however, we set in the following without loss of generality $\eta_a^{(0)}(t) = 0$. With regard to the first-order off-diagonal displacement amplitudes $\eta_{ab}^{(1)}(t)$ we easily identify antisymmetric displacement amplitudes $\eta_{ab}^{(1)}(t) = -\eta_{ba}^{(1)}(t)$ as *infinitesimal rotations* around a rotation axis perpendicular to the $r_a r_b$ plane, while symmetric off-diagonal amplitudes $\eta_{ab}^{(1)}(t) = \eta_{ba}^{(1)}(t)$ correspond to*transverse shear*. So, in the geometry under consideration density oscillations with a quadrupolar $d_{ab}$ symmetry proportional to $\rho_{ab}(t)$ can be excited by rotations or by transversal shear of the trap. Density oscillations displaying an isotropic $s$-wave symmetry proportional to $\rho_{00}(t)$, and also showing a quadrupolar $d_z^2$-wave or $d_{x^2-y^2}$-wave symmetry proportional to certain linear combinations of the diagonal amplitudes$\rho_{aa}(t)$, can be excited by a sudden change of the curvature of the trap.

According to (79) the time derivative $\hbar\frac{\partial}{\partial t}\delta s(\mathbf{r},t)$ of a phase fluctuation associated with such a density fluctuation $\delta n(\mathbf{r},t)$ is given by

$$\begin{aligned} &a,b,c \in \{x,y,z\},\\ \hbar\frac{\partial}{\partial t}\delta s(\mathbf{r},t) = -g_s\Bigg\{&\sum_{b,c}\eta_{bc}^{(1)}(t)\frac{\partial}{\partial r_b}\Bigg[(1-\varepsilon_D)n_{\mathrm{TF}}(\mathbf{r})r_c\\ &-3\varepsilon_D(\mathbf{m}\cdot\nabla_{\mathbf{r}})^2\frac{1}{4\pi}\int_{\mathbb{D}_{\mathrm{TF}}}d^3r'\frac{1}{|\mathbf{r}-\mathbf{r}'|}n_{\mathrm{TF}}(\mathbf{r}')r_c'\Bigg]\\ &+\sum_a\zeta_a(t)\frac{\partial}{\partial\lambda_a}\Bigg[(1-\varepsilon_D)n_{\mathrm{TF}}(\mathbf{r})\\ &-3\varepsilon_D(\mathbf{m}\cdot\nabla_{\mathbf{r}})^2\frac{1}{4\pi}\int_{\mathbb{D}_{\mathrm{TF}}}d^3r'\frac{1}{|\mathbf{r}-\mathbf{r}'|}n_{\mathrm{TF}}(\mathbf{r}')\Bigg]\Bigg\}. \end{aligned} \tag{85}$$

We now express the three-dimensional integrals over the Thomas-Fermi ellipsoid $\mathbb{D}_{\mathrm{TF}}$ as one-dimensional integrals using Chandrasekhar's integrals (25) and (26):

$$\frac{1}{4\pi}\int_{\mathbb{D}_{\mathrm{TF}}}d^3r'\frac{1}{|\mathbf{r}-\mathbf{r}'|}n_{\mathrm{TF}}(\mathbf{r}') = n_0\Phi_1(\mathbf{r}) \tag{86}$$

and

$$\frac{1}{4\pi}\int_{\mathbb{D}_{\mathrm{TF}}}d^3r'\frac{1}{|\mathbf{r}-\mathbf{r}'|}n_{\mathrm{TF}}(\mathbf{r}')\,r_c' = -\,n_0\frac{\lambda_c^2}{4}\frac{\partial}{\partial r_c}\Phi_2(\mathbf{r}). \tag{87}$$

The crucial trick to prove this representation for the first moment of the Thomas-Fermi density profile $n_{\mathrm{TF}}(\mathbf{r})$ is to use the identity

$$n_{\mathrm{TF}}(\mathbf{r})r_c = \left(-n_0\frac{\lambda_c^2}{4}\frac{\partial}{\partial r_c}\right)\left(1-\frac{r_x^2}{\lambda_x^2}-\frac{r_y^2}{\lambda_y^2}-\frac{r_z^2}{\lambda_z^2}\right)^2. \tag{88}$$

One finds then on partial integration a surface integral over the boundary $\partial\mathbb{D}_{\mathrm{TF}}$ and a volume integral over the Thomas-Fermi domain $\mathbb{D}_{\mathrm{TF}}$. However, the surface integral vanishes identically taking into account that $n_{\mathrm{TF}}(\mathbf{r}')\equiv 0$ for $\mathbf{r}'\in\partial\mathbb{D}_{\mathrm{TF}}$. So only the volume integral contributes, confirming the result (87).

We now rewrite the wave equation (71) for the density fluctuations,

$$\begin{aligned} 0 = \frac{\partial^2}{\partial t^2}\delta n(\mathbf{r},t) + \frac{1}{m^\star}\Bigg\{&n_{\mathrm{TF}}(\mathbf{r})\nabla_r^2\hbar\frac{\partial}{\partial t}\delta s(\mathbf{r},t)\\ &+\sum_a\frac{\partial n_{\mathrm{TF}}(\mathbf{r})}{\partial r_a}\frac{\partial}{\partial r_a}\hbar\frac{\partial}{\partial t}\delta s(\mathbf{r},t)\Bigg\}. \end{aligned} \tag{89}$$

To calculate the term $\nabla_r^2\hbar\frac{\partial}{\partial t}\delta s(\mathbf{r},t)$ we need

$$\begin{aligned} &l = 1,2,\ldots,\\ &\nabla_r^2\Phi_l(\mathbf{r}) = -\left(1-\frac{r_x^2}{\lambda_x^2}-\frac{r_y^2}{\lambda_y^2}-\frac{r_z^2}{\lambda_z^2}\right)^l. \end{aligned} \tag{90}$$

Straightforward calculations lead to

$$\begin{aligned} &\nabla_r^2\hbar\frac{\partial}{\partial t}\delta s(\mathbf{r},t)\\ &\quad= -4g_sn_0\Bigg\{(1-\varepsilon_D)\Bigg[\frac{1}{\lambda_x^2}\rho_{xx}(t)+\frac{1}{\lambda_y^2}\rho_{yy}(t)+\frac{1}{\lambda_z^2}\rho_{zz}(t)\Bigg]\\ &\qquad+3\varepsilon_D\Bigg[\frac{\cos^2(\vartheta_0)}{\lambda_z^2}\rho_{zz}(t)+\frac{\sin^2(\vartheta_0)}{\lambda_x^2}\rho_{xx}(t)\\ &\qquad+\frac{\sin(2\vartheta_0)}{2\lambda_x\lambda_z}\rho_{xz}(t)\Bigg]+\Bigg[\frac{1-\varepsilon_D}{2}\left(\frac{1}{\lambda_x^2}+\frac{1}{\lambda_y^2}+\frac{1}{\lambda_z^2}\right)\\ &\qquad+\frac{3\varepsilon_D}{2}\left(\frac{\cos^2(\vartheta_0)}{\lambda_z^2}+\frac{\sin^2(\vartheta_0)}{\lambda_x^2}\right)\Bigg]\rho_{00}(t)\Bigg\}. \end{aligned} \tag{91}$$

Likewise, we obtain

$$\begin{aligned} &a,b,c\in\{x,y,z\},\\ &\sum_a\frac{\partial n_{\mathrm{TF}}(\mathbf{r})}{\partial r_a}\frac{\partial}{\partial r_a}\hbar\frac{\partial}{\partial t}\delta s(\mathbf{r},t)\\ &\quad= -4n_0^2g_s\Bigg\{(1-\varepsilon_D)\sum_{a,c}\frac{r_a}{\lambda_a^2}\left[\frac{1}{\lambda_a^2}\eta_{ac}^{(1)}(t)+\frac{1}{\lambda_c^2}\eta_{ca}^{(1)}(t)\right]r_c\\ &\qquad-\frac{3}{2}\varepsilon_D\sum_{a,b,c}\frac{r_a}{4\lambda_a^2}\frac{\partial}{\partial r_a}\left[\eta_{bc}^{(1)}(t)\lambda_c^2\frac{\partial^2}{\partial r_b\partial r_c}(\mathbf{m}\cdot\nabla_{\mathbf{r}})^2\,\Phi_2(\mathbf{r})\right]\\ &\qquad-(1-\varepsilon_D)\sum_{a,b}\frac{\zeta_b(t)}{\lambda_b}(1+2\delta_{ab})\frac{r_a^2}{\lambda_a^4}+\frac{3}{2}\varepsilon_D\sum_{a,b}\frac{r_a}{\lambda_a^2}\frac{\partial}{\partial r_a}\\ &\qquad\times\left[\zeta_b(t)\left(-\frac{1}{\lambda_b}+\frac{\partial}{\partial\lambda_b}\right)(\mathbf{m}\cdot\nabla_{\mathbf{r}})^2\Phi_1(\mathbf{r})\right]\Bigg\}. \end{aligned} \tag{92}$$

A glance at Chandrasekhar's representation (26) for the potential functions $\Phi_l(\mathbf{r})$ of inhomogenous ellipsoids reveals that for a point $\mathbf{r}$ inside the ellipsoid $\mathbb{D}_{\mathrm{TF}}$ the potential function for $l=1$ is a fourth-order multinomial in the variables $\{1,r_x^2,r_y^2,r_z^2\}$ with coefficients proportional to the index integrals $I_a$ and $I_{ab}$, and for $l=2$ it is a sixth-order multinomial with coefficients proportional to the index integrals $I_a$, $I_{ab}$, and $I_{abc}$ (see Appendix A). The task to calculate the term (92) is therefore reduced to calculating linear combinations of derivatives of certain multinomials in the variables $\{1,r_x^2,r_y^2,r_z^2\}$:

$$\begin{aligned} &a,b,c\in\{x,y,z\},\\ &\sum_a\frac{r_a}{4\lambda_a^2}\frac{\partial}{\partial r_a}\sum_{b,c}\eta_{bc}^{(1)}(t)\lambda_c^2\frac{\partial^2}{\partial r_b\partial r_c}(\mathbf{m}\cdot\nabla_{\mathbf{r}})^2\Phi_2(\mathbf{r})\\ &\quad= -\big[F_{xx}(t)r_x^2+F_{yy}(t)r_y^2+F_{zz}(t)r_z^2+F_{xy}(t)r_xr_y\\ &\qquad+F_{yz}(t)r_yr_z+F_{xz}(t)r_xr_z\big] \end{aligned} \tag{93}$$

and

$$a,b,c \in \{x,y,z\},$$
$$\sum_a \frac{r_a}{\lambda_a^2}\frac{\partial}{\partial r_a}\sum_b \zeta_b(t)\left(-\frac{1}{\lambda_b}+\frac{\partial}{\partial \lambda_b}\right)(\mathbf{m}\cdot\nabla_{\mathbf{r}})^2\Phi_1(\mathbf{r})$$
$$= -\big[G_{xx}(t)r_x^2+G_{yy}(t)r_y^2+G_{zz}(t)r_z^2 + G_{xy}(t)r_xr_y+G_{yz}(t)r_yr_z+G_{xz}(t)r_xr_z\big], \tag{94}$$
$$G_{xy}\equiv 0\equiv G_{yz}.$$

In terms of the triple-index integrals (see Appendix A)

$$I_{abc}(\lambda_x,\lambda_y,\lambda_z)=\lambda_x\lambda_y\lambda_z\int_0^\infty \frac{du}{\sqrt{(\lambda_x^2+u)(\lambda_y^2+u)(\lambda_z^2+u)}} \times \frac{1}{(\lambda_a^2+u)(\lambda_b^2+u)(\lambda_c^2+u)},$$
$$a,b,c\in\{x,y,z\}, \tag{95}$$

the coefficients $F_{ab}(t)$ are determined as linear combinations of the displacement fluctuation amplitudes $\eta_{ab}^{(1)}(t)$, and the coefficients $G_{ab}(t)$ are determined as linear combination of the dilatation fluctuation amplitudes $\zeta_a(t)$. To evaluate the gradient terms in the wave equation (89), however, only the differences $G_{ab}(t)-F_{ab}(t)$ are needed, which can be represented as linear combinations of the fluctuation amplitudes $\rho_{ab}(t)$ defined in (82). Explicit expressions for $G_{ab}(t)-F_{ab}(t)$ in terms of the triple-index integrals $I_{abc}$ are presented in Appendix C.

Altogether we find the following second-order multinomial in the variables $\{1,\frac{r_x}{\lambda_x},\frac{r_y}{\lambda_y},\frac{r_z}{\lambda_z}\}$ for the gradient part of (89):

$$a\in\{x,y,z\},$$
$$\frac{1}{m^\star}\sum_a\left[\frac{\partial n_{\rm TF}(\mathbf{r})}{\partial r_a}\frac{\partial}{\partial r_a}\hbar\frac{\partial}{\partial t}\delta s(\mathbf{r},t)+n_{\rm TF}(\mathbf{r})\frac{\partial^2}{\partial r_a^2}\hbar\frac{\partial}{\partial t}\delta s(\mathbf{r},t)\right]$$
$$=\frac{4n_0^2g_s}{m^\star}\left[-w_{00}(t)+\sum_a w_{aa}(t)\frac{r_a^2}{\lambda_a^2}+\sum_{a<b}w_{ab}(t)\frac{r_ar_b}{\lambda_a\lambda_b}\right]. \tag{96}$$

For the coefficient proportional to unity we find

$$w_{00}(t)=\Bigg\{(1-\varepsilon_D)\left[\frac{1}{\lambda_x^2}\rho_{xx}(t)+\frac{1}{\lambda_y^2}\rho_{yy}(t)+\frac{1}{\lambda_z^2}\rho_{zz}(t)\right] +3\varepsilon_D\left[\frac{\cos^2(\vartheta_0)}{\lambda_z^2}\rho_{zz}(t)+\frac{\sin^2(\vartheta_0)}{\lambda_x^2}\rho_{xx}(t) +\frac{\sin(2\vartheta_0)}{2\lambda_x\lambda_z}\rho_{xz}(t)\right]+\left[\frac{1-\varepsilon_D}{2}\left(\frac{1}{\lambda_x^2}+\frac{1}{\lambda_y^2}+\frac{1}{\lambda_z^2}\right) +\frac{3\varepsilon_D}{2}\left(\frac{\cos^2(\vartheta_0)}{\lambda_z^2}+\frac{\sin^2(\vartheta_0)}{\lambda_x^2}\right)\right]\rho_{00}(t)\Bigg\}. \tag{97}$$

The coefficients of the diagonal terms $\frac{r_a^2}{\lambda_a^2}$ for $a\in\{x,y,z\}$ in (96) are

$$w_{aa}(t)=w_{00}(t)+(1-\varepsilon_D)\frac{1}{\lambda_a^2}[2\rho_{aa}(t)+\rho_{00}(t)] +\frac{3}{2}\varepsilon_D\lambda_a^2[G_{aa}(t)-F_{aa}(t)], \tag{98}$$

while the coefficients of the off-diagonal terms $\frac{r_ar_b}{\lambda_a\lambda_b}$ for $a,b\in\{x,y,z\}$ and $a<b$ are

$$w_{ab}(t)=(1-\varepsilon_D)\left(\frac{1}{\lambda_a^2}+\frac{1}{\lambda_b^2}\right)\rho_{ab}(t) +\frac{3}{2}\varepsilon_D\lambda_a\lambda_b\left[G_{ab}(t)-F_{ab}(t)\right]. \tag{99}$$

It follows directly from what has been said that the right-hand side of (89) represents a second-order quadratic form:

$$0\stackrel{!}{=}-\left[\frac{1}{2}\frac{\partial^2}{\partial t^2}\rho_{00}(t)+\frac{2n_0g_s}{m^\star}w_{00}(t)\right] +\sum_a\left[\frac{\partial^2}{\partial t^2}\rho_{aa}(t)+\frac{1}{2}\frac{\partial^2}{\partial t^2}\rho_{00}(t)+\frac{2n_0g_s}{m^\star}w_{aa}(t)\right]\frac{r_a^2}{\lambda_a^2} +\sum_{a<b}\left[\frac{\partial^2}{\partial t^2}\rho_{ab}(t)+\frac{2n_0g_s}{m^\star}w_{ab}(t)\right]\frac{r_ar_b}{\lambda_a\lambda_b}. \tag{100}$$

Equating the coefficients of the linearly independent basis functions $1,\frac{r_a^2}{\lambda_a^2},\frac{r_ar_b}{\lambda_a\lambda_b}$ for $a,b\in\{x,y,z\}$ to zero leads to a set of seven coupled ordinary differential equations for the sought fluctuation amplitudes $\rho_{ab}(t)$. As a matter of fact, the equation for the variable $\rho_{00}(t)$ is obsolete, because the solenoidal constraint (84) implies

$$\rho_{00}(t)=\rho_{xx}(t)+\rho_{yy}(t)+\rho_{zz}(t). \tag{101}$$

This is consistent because certain identities obeyed by the triple-index integrals $I_{abc}$ imply the following sum rule (see Appendix B):

$$\sum_a w_{aa}(t)=5w_{00}(t). \tag{102}$$

Indeed, adding the differential equations for the diagonal fluctuation amplitudes proportional to $\frac{r_a^2}{\lambda_a^2}$ leads immediately to

$$\frac{1}{2}\frac{\partial^2}{\partial t^2}\rho_{00}(t)+\frac{2n_0g_s}{m^\star}w_{00}(t)=0. \tag{103}$$

Consequently, the derivative term $\frac{\partial^2}{\partial t^2}\rho_{00}(t)$ and the term $w_{00}(t)$ in the differential equations (100) for the diagonal density fluctuation amplitudes $\rho_{aa}(t)$ cancel each other. We obtain finally the following six differential equations for six fluctuation amplitudes $\rho_{ab}(t)$:

$$a,b\in\{x,y,z\},$$
$$0=\frac{\partial^2}{\partial t^2}\rho_{aa}(t)+\frac{2n_0g^{(s)}}{m^\star}\Bigg\{(1-\varepsilon_D)\frac{1}{\lambda_a^2}\left[3\rho_{aa}(t)+\sum_{b\neq a}\rho_{bb}(t)\right] +\frac{3}{2}\varepsilon_D\lambda_a^2[G_{aa}(t)-F_{aa}(t)]\Bigg\},$$
$$0=\frac{\partial^2}{\partial t^2}\rho_{ab}(t)+\frac{2n_0g^{(s)}}{m^\star}\Bigg\{(1-\varepsilon_D)\left(\frac{1}{\lambda_a^2}+\frac{1}{\lambda_b^2}\right)\rho_{ab}(t) +\frac{3}{2}\varepsilon_D\lambda_a\lambda_b[G_{ab}(t)-F_{ab}(t)]\Bigg\}. \tag{104}$$

To determine the eigenmodes of oscillation we look for a solution of the form

$$\rho_{ab}(t)=\widehat{\rho}_{ab}(\Omega)\cos(\Omega t+\delta_\Omega), \tag{105}$$

where $\Omega$ is the eigenfrequency of the mode and $\widehat{\rho}_{ab}(\Omega)$ denotes a component of the associated eigenvector:

$$\frac{2n_0 g^{(s)}}{m^\star}\begin{bmatrix} C_{xx,xx} & C_{xx,yy} & C_{xx,zz} & C_{xx,xz} & 0 & 0 \\ C_{yy,xx} & C_{yy,yy} & C_{yy,zz} & C_{yy,xz} & 0 & 0 \\ C_{zz,xx} & C_{zz,yy} & C_{zz,zz} & C_{zz,xz} & 0 & 0 \\ C_{xz,xx} & C_{xz,yy} & C_{xz,zz} & C_{xz,xz} & 0 & 0 \\ 0 & 0 & 0 & 0 & C_{yz,yz} & C_{yz,xy} \\ 0 & 0 & 0 & 0 & C_{xy,yz} & C_{xy,xy} \end{bmatrix} \times \begin{bmatrix} \widehat{\rho}_{xx}(\Omega) \\ \widehat{\rho}_{yy}(\Omega) \\ \widehat{\rho}_{zz}(\Omega) \\ \widehat{\rho}_{xz}(\Omega) \\ \widehat{\rho}_{yz}(\Omega) \\ \widehat{\rho}_{xy}(\Omega) \end{bmatrix} = \Omega^2 \begin{bmatrix} \widehat{\rho}_{xx}(\Omega) \\ \widehat{\rho}_{yy}(\Omega) \\ \widehat{\rho}_{zz}(\Omega) \\ \widehat{\rho}_{xz}(\Omega) \\ \widehat{\rho}_{yz}(\Omega) \\ \widehat{\rho}_{xy}(\Omega) \end{bmatrix}. \tag{106}$$

We find it convenient to eliminate the interaction constant using (34):

$$2n_0\frac{g^{(s)}}{m^\star} = \frac{\omega_y^2\lambda_y^2}{1-\varepsilon_D+\frac{3\varepsilon_D}{2}\lambda_y^2[\cos^2(\vartheta_0)I_{zy}+\sin^2(\vartheta_0)I_{xy}]}. \tag{107}$$

On inspection of the coupled differential equations (104) for the coefficients $C_{ab,cd}$, explicit expressions, which are listed in Appendix C, follow.

The collective modes associated with the $4\times 4$ submatrix in (106) describe small-amplitude oscillations of the density, which are linear combinations of $s$-wave and quadrupolar $d_{x^2\text{-}y^2}$, $d_{z^2}$, and $d_{xz}$ waves, while the modes associated with the $2\times 2$ submatrix describe small-amplitude oscillations of the density consisting solely of combinations of quadrupolar $d_{yz}$ and $d_{xy}$ waves:

$$\begin{aligned}\delta n_\Omega(\mathbf{r},t) = 2n_0\Bigg[&\frac{1}{\lambda_x^2}\widehat{\rho}_{xx}(\Omega)r_x^2+\frac{1}{\lambda_y^2}\widehat{\rho}_{yy}(\Omega)r_y^2+\frac{1}{\lambda_z^2}\widehat{\rho}_{zz}(\Omega)r_z^2 \\ &-\frac{1}{2}\left(1-\frac{r_x^2}{\lambda_x^2}-\frac{r_y^2}{\lambda_y^2}-\frac{r_z^2}{\lambda_z^2}\right)\widehat{\rho}_{00}(\Omega) \\ &+\sum_{a<b}\frac{1}{\lambda_a\lambda_b}\widehat{\rho}_{ab}(\Omega)r_ar_b\Bigg]\cos(\Omega t+\delta_\Omega).\end{aligned} \tag{108}$$

By construction there holds

$$\int_{\mathbb{D}_{\mathrm{TF}}} d^3r\,\delta n_\Omega(\mathbf{r},t) = 0.$$

It is instructive to visualize the spatial dependence of the eigenmodes of small-amplitude oscillations of the density by plotting the *instantaneous* boundary of the BEC cloud when only a single mode with eigenfrequency $\Omega$ is excited. This instantaneous boundary is implicitly defined as the surface

$$n_\Omega(\mathbf{r},t) = n_{\mathrm{TF}}(\mathbf{r}) + \delta n_\Omega(\mathbf{r},t) \overset{!}{=} 0. \tag{109}$$

Finally, let us discuss which collective modes can be excited by changing the trap potential, always keeping the trap strictly harmonic while changing it. It follows directly from (82):

$$\begin{aligned} &a,b\in\{x,y,z\}, \\ \widehat{\rho}_{ab}(\Omega) = \delta_{ab}&\left[\frac{\widehat{\zeta}_a(\Omega)}{\lambda_a}-\widehat{\eta}^{(1)}_{aa}(\Omega)\right]-(1-\delta_{ab})\lambda_a\lambda_b \\ &\times\left[\frac{1}{\lambda_a^2}\widehat{\eta}^{(1)}_{ab}(\Omega_{ab})+\frac{1}{\lambda_b^2}\widehat{\eta}^{(1)}_{ba}(\Omega_{ab})\right].\end{aligned} \tag{110}$$

Sudden changes of the trap potential may excite collective density oscillations around the quantum degenerate ground state. For example, a rotation around a trap axis perpendicular to the $ab$ plane, as represented by the antisymmetric components of the tensor $\widehat{\eta}^{(1)}_{ab}$, or changes of the curvature of the trap, as represented by dilatation amplitudes $\widehat{\zeta}_a(\Omega)$, but also transversal or longitudinal shear movements of the trap, as represented by the symmetric components of the tensor $\widehat{\eta}^{(1)}_{ab}$, can be used to excite the collective modes (81) of the particle density of a trapped BEC cloud. A sudden translation of the origin of a *harmonic* trap, on the other hand, excites only the dipole modes with eigenfrequency $\Omega_a\equiv\omega_a$. It should be noted that during these collective oscillations of a spin polarized dipolar BEC cloud, as described by the density fluctuation (108), the atoms always keep the orientation of their magnetic moments strictly along the external polarizing field **B**.

### B. Pure scissors modes and mixed monopole-quadrupole excitations

Consider a harmonic trap where the principal axis $\mathbf{e}_{z,T}$ of the trap is aligned parallel to the polarizing external field **B**, i.e., $\vartheta_T=0$. In this case the off-diagonal matrix elements $C_{xy,yz}$,$C_{yz,xy}$, $C_{xz,aa}$, and $C_{aa,xz}$ vanish identically for arbitrary strength $\varepsilon_D$ of the dipole interaction parameter. There follows, then, a simpler eigenvalue problem determining the eigenmodes of the small-amplitude density oscillations:

$$\vartheta_T = 0,$$
$$\frac{2n_0 g^{(s)}}{m^\star}\begin{bmatrix} C_{xx,xx} & C_{xx,yy} & C_{xx,zz} & 0 & 0 & 0 \\ C_{yy,xx} & C_{yy,yy} & C_{yy,zz} & 0 & 0 & 0 \\ C_{zz,xx} & C_{zz,yy} & C_{zz,zz} & 0 & 0 & 0 \\ 0 & 0 & 0 & C_{xz,xz} & 0 & 0 \\ 0 & 0 & 0 & 0 & C_{yz,yz} & 0 \\ 0 & 0 & 0 & 0 & 0 & C_{xy,xy} \end{bmatrix} \times \begin{bmatrix} \widehat{\rho}_{xx}(\Omega) \\ \widehat{\rho}_{yy}(\Omega) \\ \widehat{\rho}_{zz}(\Omega) \\ \widehat{\rho}_{xz}(\Omega) \\ \widehat{\rho}_{yz}(\Omega) \\ \widehat{\rho}_{xy}(\Omega) \end{bmatrix} = \Omega^2 \begin{bmatrix} \widehat{\rho}_{xx}(\Omega) \\ \widehat{\rho}_{yy}(\Omega) \\ \widehat{\rho}_{zz}(\Omega) \\ \widehat{\rho}_{xz}(\Omega) \\ \widehat{\rho}_{yz}(\Omega) \\ \widehat{\rho}_{xy}(\Omega) \end{bmatrix}. \tag{111}$$

Three modes with indices $a\neq b$ display a pure quadrupolar $d_{xz}$, $d_{yz}$, and $d_{xy}$ symmetry. Also there exists a mixed symmetry coupling between two basis functions with $d$-wave symmetry and one basis function with $s$-wave symmetry. This is reminiscent of the symmetry of the discrete group $D_{4h}$ lifting the fivefold degeneracy of the $l=2$ spherical harmonics into three one-dimensional manifolds, namely $A_{1g}$, $B_{1g}$, and $B_{2g}$, and a two-dimensional $E_g$ manifold. We refer to the one-dimensional (trivial) representation of the isotropic basis function with $s$-wave symmetry as $a_{1g}$.

In the geometry under consideration the $E_g$ manifold is spanned by basis functions with $d_{yz}$ and $d_{xy}$ symmetry, while $B_{2g}$ is spanned by a single basis function with $d_{xz}$ symmetry and $B_{1g}$ is spanned by a single basis function with $d_{x^2-y^2}$ symmetry. The one-dimensional manifold $A_{1g}$ represents a fixed linear combination of basis elements with $d_{z^2}$- and $s$-wave symmetry. So the upper $3 \times 3$ block in (111) describes a coupling between members of the $a_{1g}$, $A_{1g}$, and $B_{1g}$ manifolds. For $\omega_x = \omega_y \neq \omega_z$ there exists a pure $B_{1g}$ mode and two coupled modes with mixed $a_{1g}$ and $A_{1g}$ symmetry.

The eigenfrequencies of the $B_{2g}$ and $E_g$ modes are obtained from the diagonal matrix elements $C_{xz,xz}$, $C_{yz,yz}$, and $C_{xy,xy}$, taking the limit $\vartheta_0 \to 0$:

$$\Omega_{xz}^2 = \omega_y^2 \left( \frac{\lambda_y^2}{\lambda_x^2} + \frac{\lambda_y^2}{\lambda_z^2} \right) \frac{(1-\varepsilon_D) + \frac{9}{2}\varepsilon_D \frac{\lambda_x^2}{\lambda_z^2} \overline{I}_{xzz}}{1 - \varepsilon_D + \frac{3\varepsilon_D}{2}\frac{\lambda_y^2}{\lambda_z^2}\overline{I}_{zy}},$$
$$\Omega_{yz}^2 = \omega_y^2 \left( 1 + \frac{\lambda_y^2}{\lambda_z^2} \right) \frac{(1-\varepsilon_D) + \frac{9}{2}\varepsilon_D \frac{\lambda_y^2}{\lambda_z^2} \overline{I}_{yzz}}{1 - \varepsilon_D + \frac{3\varepsilon_D}{2}\frac{\lambda_y^2}{\lambda_z^2}\overline{I}_{zy}}, \qquad (112)$$
$$\Omega_{xy}^2 = \omega_y^2 \left( 1 + \frac{\lambda_y^2}{\lambda_x^2} \right) \frac{(1-\varepsilon_D) + \frac{3}{2}\varepsilon_D \frac{\lambda_x^2}{\lambda_z^2}\frac{\lambda_y^2}{\lambda_z^2} \overline{I}_{xyz}}{1 - \varepsilon_D + \frac{3\varepsilon_D}{2}\frac{\lambda_y^2}{\lambda_z^2}\overline{I}_{zy}}.$$

The spatial variation of the associated density fluctuation of these modes is purely two dimensional:

$$a,b \in \{x,y,z\},$$
$$a \neq b,$$
$$\widehat{\rho}_{a'b'}(\Omega_{ab}) = \delta_{aa'}\delta_{bb'}, \qquad (113)$$
$$\delta n_{\Omega_{ab}}(\mathbf{r},t) = 2n_0 \widehat{\rho}_{ab}(\Omega_{ab}) \frac{r_a r_b}{\lambda_a \lambda_b} \cos(\Omega_{ab} t + \delta_{\Omega_{ab}}).$$

In the limit $\varepsilon_D \to 0$ it is found that $\frac{\lambda_a}{\lambda_b} \to \frac{\omega_b}{\omega_a}$. Then one obtains for a BEC without dipole-dipole interactions confined inside a harmonic trap

$$a \neq b,$$
$$\lim_{\varepsilon_D \to 0} \Omega_{ab} = \sqrt{\omega_a^2 + \omega_b^2}. \qquad (114)$$

These are the so-called scissors modes first predicted by Guéry-Odelin and Stringari [12] and then observed in experiments [17,18].

In order to specify conditions that enable excitation of the scissors modes (113) for a dipolar BEC cloud confined in a harmonic trap we point out that the components $\widehat{\rho}_{a'b'}(\Omega_{ab}) = \delta_{aa'}\delta_{bb'}$ of the eigenvectors of the respective modes are connected to the off-diagonal displacement amplitudes $\widehat{\eta}_{ab}^{(1)}$, see (82), by

$$a \neq b,$$
$$\widehat{\rho}_{ab}(\Omega_{ab}) = -\lambda_a \lambda_b \left[ \frac{1}{\lambda_a^2} \widehat{\eta}_{ab}^{(1)}(\Omega_{ab}) + \frac{1}{\lambda_b^2} \widehat{\eta}_{ba}^{(1)}(\Omega_{ab}) \right]. \qquad (115)$$

For an infinitesimal rotation of the BEC cloud around one of its symmetry axes, say $\mathbf{e}_{c,0} = \mathbf{e}_{a,0} \wedge \mathbf{e}_{b,0}$, the associated displacement amplitude is antisymmetric, $\widehat{\eta}_{ab}^{(1)} = -\widehat{\eta}_{ba}^{(1)}$. So one recognizes immediately that in the highly symmetric case $\vartheta_T = 0$ a scissors mode with amplitude $\widehat{\rho}_{ab}(\Omega_{ab})$ cannot be excited by a rotation around a principal axis of the BEC cloud perpendicular to the $ab$ plane, if the semiaxes $\lambda_a$ and $\lambda_b$ of the BEC cloud in that plane are equal, i.e., $\lambda_a = \lambda_b$. However, even then a scissors mode may get excited by a sudden *tranverse shear* movement of the trap as described by a symmetric displacement amplitude $\widehat{\eta}_{ab}^{(1)} = \widehat{\eta}_{ba}^{(1)}$. If the BEC is confined inside a harmonic trap with triaxial symmetry, one may always excite the scissors modes $\Omega_{ab}$ by a sudden infinitesimal rotation of the trap potential around a symmetry axis perpendicular to the respective $ab$ plane.

Let us now discuss the coupled modes corresponding to the $3 \times 3$ sub-block in (111). These are small-amplitude oscillations of the density that are linear combinations of the three diagonal amplitudes $\widehat{\rho}_{aa}(\Omega)$. In the limit $\varepsilon_D \to 0$ the corresponding eigenfrequencies and eigenvectors of the triplet of coupled modes can be obtained by solving a cubic equation for the frequencies $\Omega^{(0)}$:

$$\begin{bmatrix} 3\omega_x^2 & \omega_x^2 & \omega_x^2 \\ \omega_y^2 & 3\omega_y^2 & \omega_y^2 \\ \omega_z^2 & \omega_z^2 & 3\omega_z^2 \end{bmatrix} \begin{bmatrix} \widehat{\rho}_{xx}(\Omega^{(0)}) \\ \widehat{\rho}_{yy}(\Omega^{(0)}) \\ \widehat{\rho}_{zz}(\Omega^{(0)}) \end{bmatrix} = [\Omega^{(0)}]^2 \begin{bmatrix} \widehat{\rho}_{xx}(\Omega^{(0)}) \\ \widehat{\rho}_{yy}(\Omega^{(0)}) \\ \widehat{\rho}_{zz}(\Omega^{(0)}) \end{bmatrix}. \qquad (116)$$

One easily sees that for a triaxial trap the eigenmodes of this triplet are mixtures of basis functions with isotropic $s$-wave and quadrupolar $d_{z^2}$-wave and $d_{x^2-y^2}$-wave symmetry, respectively.

When the harmonic trap has a uniaxial (cylindrical) symmetry, $\omega_z \neq \omega_y = \omega_x = \omega_\perp$, simple analytic formulas for the eigenfrequencies and eigenmodes of the density oscillations of a BEC cloud can be derived from (116) that apply for $\varepsilon_D = 0$. One easily obtains the well-known results first derived by Stringari for the three eigenfrequencies $\Omega_{x^2-y^2}^{(0)}$, $\Omega_s^{(0)}$, $\Omega_{z^2}^{(0)}$ [19]. In Appendix D we present a detailed discussion of these modes as a function of the anisotropy ratio

$$\nu = \frac{\omega_z}{\omega_\perp}. \qquad (117)$$

### C. Spherical harmonic trap

For the special case of a *spherical* harmonic trap, say, with trap frequency $\omega_a \equiv \omega$, setting $\lambda_a^{(0)} \equiv \Lambda$, we immediately find from (116) for a BEC without dipole-dipole interaction (see Appendix D)

$$\Omega = \Omega_{x^2-y^2}^{(0)} = \sqrt{2}\omega,$$
$$\delta n_\Omega(\mathbf{r},t) = 2n_0 \cos(\Omega t + \delta_\Omega) \frac{r_x^2 - r_y^2}{\Lambda^2}, \qquad (118)$$

$$\Omega \equiv \Omega_+^{(0)} = \sqrt{5}\omega,$$
$$\delta n_\Omega(\mathbf{r},t) = n_0 \cos(\Omega t + \delta_\Omega) \left( 5\frac{r_x^2 + r_y^2 + r_z^2}{\Lambda^2} - 3 \right), \qquad (119)$$

$$\Omega = \Omega_-^{(0)} = \sqrt{2}\omega,$$
$$\delta n_\Omega(\mathbf{r},t) = n_0 \cos(\Omega t + \delta_\Omega) \frac{2r_z^2 - r_x^2 - r_y^2}{\Lambda^2}. \qquad (120)$$

So for $\varepsilon_D = 0$, a BEC cloud confined inside a harmonic *spherical* trap may get excited as an $s$-wave breather mode with frequency $\Omega_+^{(0)} = \sqrt{5}\omega$, or as a quintuplet of degenerate modes with quadrupolar symmetry and frequency $\Omega_{x^2\text{-}y^2}^{(0)} = \Omega_-^{(0)} = \Omega_{xz}^{(0)} = \Omega_{yz}^{(0)} = \Omega_{xy}^{(0)} = \sqrt{2}\omega$, namely three scissors modes with $d_{xz}$, $d_{yz}$, and $d_{xy}$ symmetry and two modes with $d_{x^2\text{-}y^2}$ and $d_{z^2}$ symmetry.

Next we take into account the effect of the dipole-dipole interaction. According to (49) for $\varepsilon_D > 0$, the ground state of a spin-polarized dipolar BEC cloud confined in a *spherical* trap with trap frequency $\omega_a \equiv \omega$ displays uniaxial symmetry along the direction of the magnetic field $\mathbf{B}$, so $\lambda_x = \lambda_y < \lambda_z$. Let us check if, for $\varepsilon_D \neq 0$, the modes of a dipolar BEC cloud confined in a *spherical* trap are qualitatively similar to the aforementioned collective modes of a BEC cloud without dipole-dipole interaction, $\varepsilon_D = 0$, for the case of a prolate trap with *cylindrical* symmetry: $\omega_z < \omega_y = \omega_x$.

Indeed, for a spherical trap with trap frequency $\omega$ we have $\vartheta_0 = 0$, so all matrix elements in (111) can be expressed in terms of the following expressions:

$$\begin{aligned} A &= \frac{1-\varepsilon_D + \frac{3}{2}\varepsilon_D \frac{\lambda_y^4}{\lambda_z^4}\overline{I}_{yyz}}{1-\varepsilon_D + \frac{3\varepsilon_D}{2}\frac{\lambda_y^2}{\lambda_z^2}\overline{I}_{zy}},\\ B &= \frac{1-\varepsilon_D + \frac{9}{2}\varepsilon_D \frac{\lambda_y^2}{\lambda_z^2}\overline{I}_{yzz}}{1-\varepsilon_D + \frac{3\varepsilon_D}{2}\frac{\lambda_y^2}{\lambda_z^2}\overline{I}_{zy}},\\ C &= \frac{1-\varepsilon_D + \frac{15}{2}\varepsilon_D \overline{I}_{zzz}}{1-\varepsilon_D + \frac{3\varepsilon_D}{2}\frac{\lambda_y^2}{\lambda_z^2}\overline{I}_{zy}}. \end{aligned} \tag{121}$$

It follows then from (111) that

$$\begin{aligned} \Omega_{xz}^2 = \Omega_{yz}^2 &= \left(1+\frac{\lambda_y^2}{\lambda_z^2}\right)\omega^2 B,\\ \Omega_{xy}^2 &= 2\omega^2 A,\\ \widehat{\rho}_{a'b'}(\Omega_{ab}) &= \delta_{aa'}\delta_{bb'}. \end{aligned} \tag{122}$$

So the scissors modes with $d_{xz}$ and $d_{yz}$ symmetry remain degenerate.

For $\varepsilon_D \neq 0$ the $3\times 3$ sub-block in (111) represents a triplet of coupled modes. For the case of a dipolar BEC confined in a *spherical* trap there follows

$$\omega^2 \begin{bmatrix} 3A & A & B\\ A & 3A & B\\ \frac{\lambda_y^2}{\lambda_z^2}B & \frac{\lambda_y^2}{\lambda_z^2}B & 3\frac{\lambda_y^2}{\lambda_z^2}C \end{bmatrix} \begin{bmatrix} \widehat{\rho}_{xx}(\Omega)\\ \widehat{\rho}_{yy}(\Omega)\\ \widehat{\rho}_{zz}(\Omega) \end{bmatrix} = \Omega^2 \begin{bmatrix} \widehat{\rho}_{xx}(\Omega)\\ \widehat{\rho}_{yy}(\Omega)\\ \widehat{\rho}_{zz}(\Omega) \end{bmatrix}. \tag{123}$$

It is easy to see that the mode with quadrupolar $d_{x^2\text{-}y^2}$ symmetry remains an exact eigenstate for $\varepsilon_D \neq 0$:

$$\begin{aligned} \Omega_{x^2\text{-}y^2}^2 &= 2\omega^2 A = \Omega_{xy}^2,\\ \begin{bmatrix} \widehat{\rho}_{xx}(\Omega_{x^2\text{-}y^2})\\ \widehat{\rho}_{yy}(\Omega_{x^2\text{-}y^2})\\ \widehat{\rho}_{zz}(\Omega_{x^2\text{-}y^2}) \end{bmatrix} &= \begin{bmatrix} 1\\ -1\\ 0 \end{bmatrix}. \end{aligned} \tag{124}$$

So for $\varepsilon_D \neq 0$ the quadrupolar modes with $d_{x^2\text{-}y^2}$ and $d_{xy}$ symmetry remain degenerate for the case of a spherical harmonic trap.

Next we show that the isotropic breather mode of a dipolar BEC inside a spherical trap with frequency $\omega$ is an eigenstate of the small-amplitude density oscillations of the BEC cloud, displaying an exact $s$-wave symmetry for any value of the dipole interaction strength $\varepsilon_D \neq 0$:

$$\begin{aligned} \Omega_s^2 &= 5\omega^2,\\ \begin{bmatrix} \widehat{\rho}_{xx}(\Omega_s)\\ \widehat{\rho}_{yy}(\Omega_s)\\ \widehat{\rho}_{zz}(\Omega_s) \end{bmatrix} &= \begin{bmatrix} 1\\ 1\\ 1 \end{bmatrix}. \end{aligned} \tag{125}$$

If this claim was correct, then it should be true that

$$\begin{aligned} 4A + B &= 5,\\ \frac{\lambda_y^2}{\lambda_z^2}(2B+3C) &= 5. \end{aligned} \tag{126}$$

Indeed, making use of identities (A7) and (A8) obeyed by the triple-index integrals $I_{abc}$, we see that

$$4\frac{\lambda_y^2}{\lambda_z^2}\overline{I}_{yyz} + 3\overline{I}_{yzz} = 5\overline{I}_{zy}, \tag{127}$$

$$\begin{aligned} 4A + B &= 4\frac{1-\varepsilon_D + \frac{3}{2}\varepsilon_D \frac{\lambda_y^4}{\lambda_z^4}\overline{I}_{yyz}}{1-\varepsilon_D + \frac{3\varepsilon_D}{2}\frac{\lambda_y^2}{\lambda_z^2}\overline{I}_{zy}} + \frac{1-\varepsilon_D + \frac{9}{2}\varepsilon_D \frac{\lambda_y^2}{\lambda_z^2}\overline{I}_{yzz}}{1-\varepsilon_D + \frac{3\varepsilon_D}{2}\frac{\lambda_y^2}{\lambda_z^2}\overline{I}_{zy}}\\ &= \frac{5(1-\varepsilon_D) + \frac{3}{2}\varepsilon_D\frac{\lambda_y^2}{\lambda_z^2}\left(4\frac{\lambda_y^2}{\lambda_z^2}\overline{I}_{yyz} + 3\overline{I}_{yzz}\right)}{1-\varepsilon_D + \frac{3\varepsilon_D}{2}\frac{\lambda_y^2}{\lambda_z^2}\overline{I}_{zy}}\\ &= 5, \end{aligned}$$

and

$$5\overline{I}_{zzz} + 2\frac{\lambda_y^2}{\lambda_z^2}\overline{I}_{yzz} = 5\overline{I}_{zz}, \tag{128}$$

$$\begin{aligned} \frac{\lambda_y^2}{\lambda_z^2}(2B+3C) &= 2\frac{\lambda_y^2}{\lambda_z^2}\frac{1-\varepsilon_D + \frac{9}{2}\varepsilon_D\frac{\lambda_y^2}{\lambda_z^2}\overline{I}_{yzz}}{1-\varepsilon_D + \frac{3\varepsilon_D}{2}\frac{\lambda_y^2}{\lambda_z^2}\overline{I}_{zy}}\\ &\quad + 3\frac{\lambda_y^2}{\lambda_z^2}\frac{1-\varepsilon_D + \frac{15}{2}\varepsilon_D\overline{I}_{zzz}}{1-\varepsilon_D + \frac{3\varepsilon_D}{2}\frac{\lambda_y^2}{\lambda_z^2}\overline{I}_{zy}}\\ &= \frac{\lambda_y^2}{\lambda_z^2}\frac{5(1-\varepsilon_D) + \frac{9}{2}\varepsilon_D\left(2\frac{\lambda_y^2}{\lambda_z^2}\overline{I}_{yzz} + 5\overline{I}_{zzz}\right)}{1-\varepsilon_D + \frac{3\varepsilon_D}{2}\frac{\lambda_y^2}{\lambda_z^2}\overline{I}_{zy}}\\ &= 5\frac{\lambda_y^2}{\lambda_z^2}\frac{1-\varepsilon_D + \frac{9}{2}\varepsilon_D\overline{I}_{zz}}{1-\varepsilon_D + \frac{3\varepsilon_D}{2}\frac{\lambda_y^2}{\lambda_z^2}\overline{I}_{zy}}\\ &= 5. \end{aligned}$$

The last line follows because the self-consistency equation (46) implies for the case of a *spherical* trap

$$\frac{\lambda_y^2}{\lambda_z^2} = \frac{1-\varepsilon_D + \frac{3\varepsilon_D}{2}\frac{\lambda_y^2}{\lambda_z^2}\overline{I}_{yz}}{1-\varepsilon_D + \frac{9\varepsilon_D}{2}\overline{I}_{zz}}. \tag{129}$$

Because for a finite value $\varepsilon_D > 0$ a spin-polarized dipolar BEC cloud confined in a spherical harmonic trap with frequency $\omega$ has the shape of an uniaxial (prolate) ellipsoid orientated parallel to $\mathbf{B}$, so $\lambda_x = \lambda_y < \lambda_z$, we find it remarkable that the isotropic breather mode (125) remains an *exact* eigenmode of the small-amplitude density fluctuations with $s$-wave symmetry, oscilllating at a *constant* frequency $\Omega_s = \sqrt{5}\omega$ that is *independent* on the value of the dipole interaction strength for $-\frac{1}{2} < \varepsilon_D < 1$.

Knowledge of two eigenvalues is sufficient to determine the third one from the trace of the coefficient matrix in (123):

$$\Omega_s^2 + \Omega_{x^2\text{-}y^2}^2 + \Omega_{z^2}^2 = 6\omega^2\left(A + \frac{\lambda_y^2}{2\lambda_z^2}C\right). \tag{130}$$

This leads for the eigenfrequency and the eigenvector of the density oscillations with a predominant $d_{z^2}$ symmetry to the result

$$\Omega_{z^2}^2 = \omega^2\left(4A + 3\frac{\lambda_y^2}{\lambda_z^2}C - 5\right),$$
$$\begin{bmatrix}\widehat{\rho}_{xx}(\Omega_{z^2})\\ \widehat{\rho}_{yy}(\Omega_{z^2})\\ \widehat{\rho}_{zz}(\Omega_{z^2})\end{bmatrix} = \begin{bmatrix}-\frac{\lambda_z^2}{\lambda_y^2}\frac{5-4A}{2B}\\ -\frac{\lambda_z^2}{\lambda_y^2}\frac{5-4A}{2B}\\ 1\end{bmatrix}. \tag{131}$$

It follows from what has been said that the degeneracy of the small-amplitude collective modes of a dipolar BEC cloud confined in a spherical harmonic trap is only partially lifted for $\varepsilon_D \neq 0$. For a spherical trap the modes with $d_{x^2\text{-}y^2}$ and $d_{xy}$ symmetry, and the modes with $d_{yz}$ and $d_{xz}$ symmetry, remain degenerate, irrespective of the value of the dipole interaction $\varepsilon_D$. In Fig. 6 we plot the collective mode frequencies $\Omega_s$, $\Omega_{z^2}$, $\Omega_{xy}$, and $\Omega_{xz}$ vs the interaction strength parameter $\varepsilon_D$. For small $|\varepsilon_D|$the splitting of the quadrupolar modes $\Omega_{z^2}$, $\Omega_{xy}$, and $\Omega_{xz}$ is weak. Most remarkably, the breather mode $\Omega_s$ displays for $-\frac{1}{2} < \varepsilon_D < 1$ an exact $s$-wave symmetry, the eigenfrequency assuming a constant value $\Omega_s = \sqrt{5}\omega$, even though for $\varepsilon_D \neq 0$ the shape of the ground state is not isotropic.

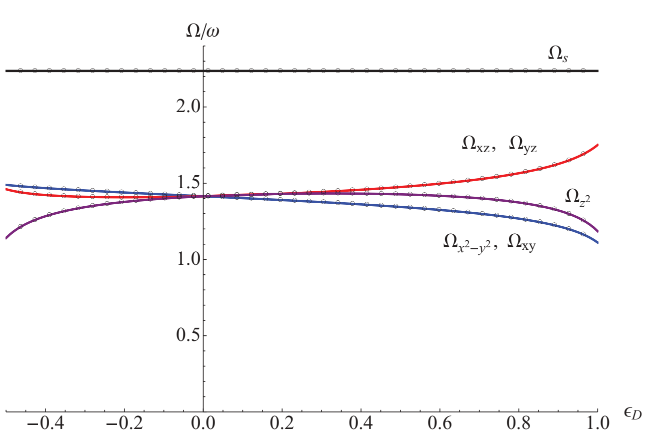


FIG. 6. (Color online) Eigenfrequencies $\Omega_s$, $\Omega_{z^2}$, $\Omega_{xz} = \Omega_{yz}$. and $\Omega_{xy} = \Omega_{x^2\text{-}y^2}$ of small-amplitude density oscillations of BEC cloud vs dipole interaction strength $\varepsilon_D$ for a *spherical* harmonic trap with trap frequeny $\omega$.

The following reason can be given for the breather mode frequency of a dipolar BEC being independent on the dipole interaction strength $\varepsilon_D$ for an *isotropic* harmonic trap. The microscopic Hamiltonian of a dipolar interacting gas cloud consisting of $N$ atoms is

$$\begin{aligned}
\widehat{H} &= \widehat{H}_{\text{kin}} + \widehat{H}_{\text{pot}} + \widehat{H}_{\text{int}},\\
\widehat{H}_{\text{kin}} &= \sum_{n=1}^{N}\frac{1}{2m^\star}\sum_{a\in\{x,y,z\}} p_a^{(n)}p_a^{(n)},\\
\widehat{H}_{\text{pot}} &= \sum_{n=1}^{N}\frac{m^\star\omega^2}{2}\sum_{a\in\{x,y,z\}} r_a^{(n)}r_a^{(n)},\\
\widehat{H}_{\text{int}} &= \frac{1}{2}\sum_{\substack{n,n'=1\\ n'\neq n}}^{N} U(\mathbf{r}^{(n)},\mathbf{r}^{(n')}).
\end{aligned} \tag{132}$$

The breather mode (or monopole mode) of small-amplitude collective density oscillations of such an atom cloud may get excited by a sudden change of the curvature of the trap potential, say, by changing the trap frequency $\omega \to \omega + \delta\omega$. The associated excitation operator is

$$\delta\widehat{V} = m^\star\omega\delta\omega\sum_{n=1}^{N}\sum_{a\in\{x,y,z\}} r_a^{(n)}r_a^{(n)}. \tag{133}$$

It is important to realize that the interaction potential $U(\mathbf{r}^{(n)},\mathbf{r}^{(n')})$ for the spin-polarized dipolar BEC in (4) transforms under a scaling transformation $\mathbf{r} \to \Lambda\mathbf{r}$ like a homogeneous function with scaling degree $-3$:

$$U(\Lambda\mathbf{r}^{(n)},\Lambda\mathbf{r}^{(n')}) = \Lambda^{-3}U(\mathbf{r}^{(n)},\mathbf{r}^{(n')}). \tag{134}$$

Together with Newton's law of action and reaction (78) this implies

$$[[\delta\widehat{V},\widehat{H}],\widehat{H}] = 2\hbar^2\omega\delta\omega\,(2\widehat{H}_{\text{pot}} - 2\widehat{H}_{\text{kin}} - 3\widehat{H}_{\text{int}}). \tag{135}$$

If $\Psi_0$ denotes the ground state and $E_0$ the ground-state energy of the system under consideration, there holds

$$\begin{aligned}
0 &= \langle\Psi_0,([\delta\widehat{V},\widehat{H}]E_0 - E_0[\delta\widehat{V},\widehat{H}])\Psi_0\rangle\\
&= \langle\Psi_0,[[\delta\widehat{V},\widehat{H}],\widehat{H}]\Psi_0\rangle.
\end{aligned} \tag{136}$$

Inserting the double commutator (135), it is found that the full interaction energy of a dipolar interacting BEC in the ground state is proportional to a difference of kinetic and potential energy only:

$$\langle\widehat{H}_{\text{int}}\rangle_{\Psi_0} = \tfrac{2}{3}\langle\widehat{H}_{\text{pot}}\rangle_{\Psi_0} - \tfrac{2}{3}\langle\widehat{H}_{\text{kin}}\rangle_{\Psi_0}. \tag{137}$$

It should be emphasized that if in (4) the scaling degree of the long-ranged interaction (6) under $\mathbf{r} \to \Lambda\mathbf{r}$ differed from the scaling degree $-3$ of the short-ranged $s$-wave contact interaction (5), the derived virial identity (137) would not apply.

Next we employ a well-known sum rule [19,20] providing an upper bound for the low-lying excitation energies $E_1 - E_0$

that can be excited by a Hermitian perturbation operator $\delta\widehat{V}$:

$$(E_1 - E_0)^2 \leqslant \frac{\langle\Psi_0,[[\delta\widehat{V},\widehat{H}],[[\delta\widehat{V},\widehat{H}],\widehat{H}]]\Psi_0\rangle}{\langle\Psi_0,[\delta\widehat{V},[\widehat{H},\delta\widehat{V}]]\Psi_0\rangle}. \quad (138)$$

For the operator $\delta\widehat{V}$ exciting the breather mode [see (133)], it is found that

$$[\delta\widehat{V},[\widehat{H},\delta\widehat{V}]] = 8\hbar^2(\delta\omega)^2\widehat{H}_{\text{pot}} \quad (139)$$

and

$$[[\delta\widehat{V},\widehat{H}],[[\delta\widehat{V},\widehat{H}],\widehat{H}]] = 4\hbar^4(\omega\delta\omega)^2(4\widehat{H}_{\text{pot}} + 4\widehat{H}_{\text{kin}} + 9\widehat{H}_{\text{int}}). \quad (140)$$

From what has been said there follows now for the frequency $\Omega_s$ of the breather mode an upper bound

$$(\hbar\Omega_s)^2 \leqslant (\hbar\omega)^2\frac{2\langle\widehat{H}_{\text{pot}}\rangle_{\Psi_0} + 2\langle\widehat{H}_{\text{kin}}\rangle_{\Psi_0} + \frac{9}{2}\langle\widehat{H}_{\text{int}}\rangle_{\Psi_0}}{\langle\widehat{H}_{\text{pot}}\rangle_{\Psi_0}} = (\hbar\omega)^2\left(5 - \frac{\langle\widehat{H}_{\text{kin}}\rangle_{\Psi_0}}{\langle\widehat{H}_{\text{pot}}\rangle_{\Psi_0}}\right). \quad (141)$$

For the optimized ground state (1) of a BEC, as constructed from a solution to the Gross-Pitaevskii equation (2), the ratio of kinetic to potential energy scales as

$$\frac{\langle\widehat{H}_{\text{kin}}\rangle_{\Psi_0}}{\langle\widehat{H}_{\text{pot}}\rangle_{\Psi_0}} = o\left(N^{-\frac{4}{5}}\right). \quad (142)$$

So, in the Thomas-Fermi approximation, the derived upper bound for the breather mode frequency is indeed independent of the strength of the dipole-dipole interaction parameter $\varepsilon_D$. The fact that this upper bound actually coincides with the previously derived result $\Omega_s = \sqrt{5}\omega$, which was obtained solving the eigenvalue problem (123) for the small-amplitude collective modes of density oscillations, suggests that the spectral weight of the mode is indeed exhausted by the specified excitation operator $\delta\widehat{V}$ (133) of the monopole mode.

It is instructive to visualize the spatial variation of the associated density eigenmodes $\delta n_\Omega(\mathbf{r},t)$ by plotting the instantaneous surface of the BEC cloud as defined by (109). In Fig. 7 and in Fig. 8 these eigenmodes are plotted at stroboscopic times $t = 0, t = \frac{\pi}{2\Omega}$, and $t = \frac{\pi}{\Omega}$, corresponding to maximal, zero, and minimal deviation from the boundary $\partial\mathbb{D}_{\text{TF}}$ of the ground-state cloud $\mathbb{D}_{\text{TF}}$, respectively. The plots shown are based on a self-consistent calculation of the ground-state cloud for a dipole interaction strength parameter $\varepsilon_D = 0.7$, assuming that the BEC cloud is confined inside a *spherical* harmonic trap with trap frequency $\omega$. The amplitudes of the respective eigenmodes $\delta n_\Omega(\mathbf{r},t)$ of the density fluctuation have been scaled by a suitable factor for each mode separately to make the typical shapes better visible. The $s$-wave breather mode is clearly distinguished in its appearance from the three characteristic scissors modes with their $d_{xz}$-, $d_{yz}$-, and $d_{xy}$-wave symmetry and the $d_{x^2-y^2}$-wave and $d_z^2$-wave quadrupolar modes.

### D. Spectrum of low-lying excitations for the case $\vartheta_T = 0$

We now discuss the collective density oscillations of a dipolar BEC cloud confined in a triaxial harmonic trap in the highly symmetric case, when the principal axis $\mathbf{e}_{z,T}$ of the trap is orientated collinear to the spin-polarizing magnetic field $\mathbf{B}$, so $\vartheta_T = 0$. In Figs. 9 and 10 the collective mode frequencies $\Omega$ corresponding to the solution of the eigenvalue problem (111) are plotted vs the dipole interaction strength $\varepsilon_D$. Shown are three scissors modes with $d_{xz}$-, $d_{yz}$-, and $d_{xy}$-wave symmetry and three hybridized modes combined from basis elements with $s$-wave, $d_{z^2}$-wave, and $d_{x^2-y^2}$-wave symmetry. The anisotropy ratio chosen is $\omega_x$:$\omega_y$:$\omega_z$ = 712:128:942 in Fig. 9, and in reverse order, $\omega_x$:$\omega_y$:$\omega_z$ = 942:128:712 in Fig. 10, respectively.

There exists fair agreement between our exact analytical results and the numerical results obtained in Ref. [21], which are based on the method of solving Newton equations of motion for time-dependent Thomas-Fermi radii. As is evident from (110), small-amplitude fluctuations of the Thomas-Fermi radii are described in our approach by the dilatation amplitudes $\widehat{\zeta}_a(t)$. However, in the highly symmetric case $\vartheta_T = 0$, these dilatation amplitudes couple only to the diagonal basis elements of the tensor $\widehat{\rho}_{ab}$:

$$\widehat{\rho}_{aa}(\Omega) = \frac{\widehat{\zeta}_a(\Omega)}{\lambda_a} - \widehat{\eta}^{(1)}_{aa}(\Omega). \quad (143)$$

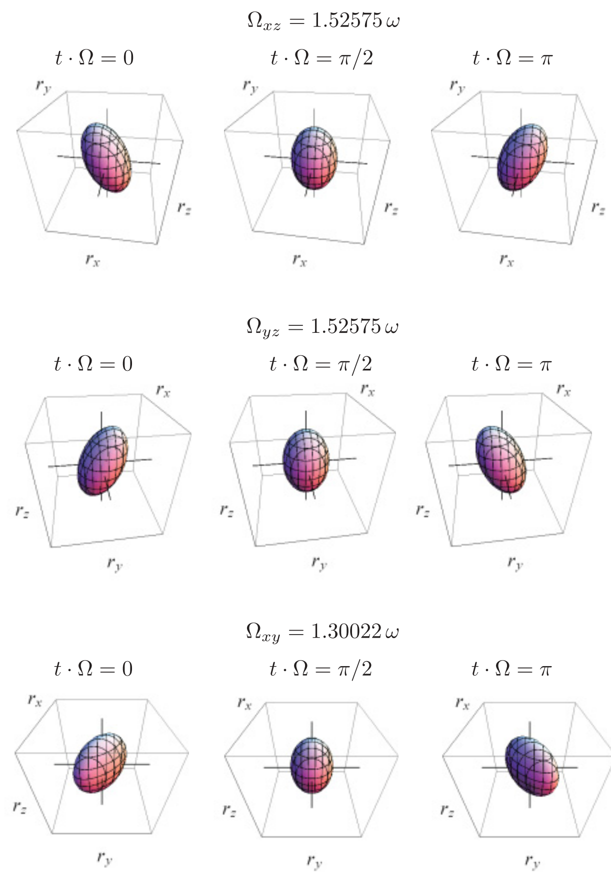


FIG. 7. (Color online) Visualization of density fluctuations $n_\Omega(\mathbf{r},t) = n_{\text{TF}}(\mathbf{r}) + \delta n_\Omega(\mathbf{r},t)$ of scissors modes for dipolar BEC cloud confined inside a spherical trap for a dipole interaction strength $\varepsilon_D = 0.7$.

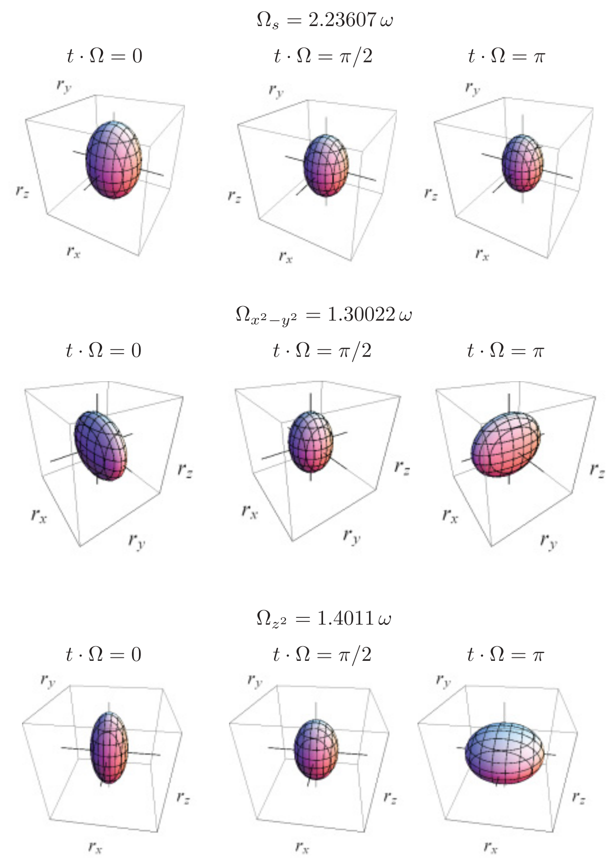


FIG. 8. (Color online) Visualization of density fluctuations $n_\Omega(\mathbf{r},t) = n_{\mathrm{TF}}(\mathbf{r}) + \delta n_\Omega(\mathbf{r},t)$ of dipolar BEC cloud confined inside a spherical trap for a dipole interaction strength $\varepsilon_D = 0.7$. (First row) Isotropic breather mode $\Omega_s$; (second row) quadrupolar mode $\Omega_{x^2-y^2}$; (third row) quadrupolar mode $\Omega_{z^2}$.

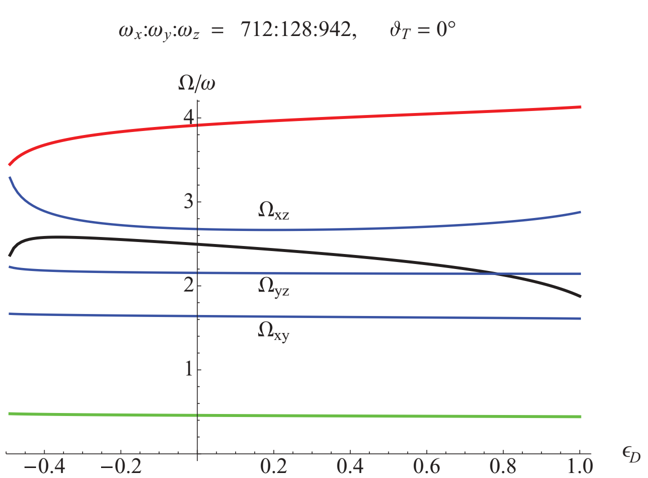


FIG. 9. (Color online) Eigenfrequencies of small-amplitude collective modes combining isotropic $s$-wave and quadrupolar $d$-wave basis elements vs the dipole interaction strength $\varepsilon_D$ for a dipolar BEC cloud confined in a harmonic trap with the anisotropy ratio $\omega_x{:}\omega_y{:}\omega_z = 712{:}128{:}942$ in the highly symmetric case $\vartheta_T = 0$. Displayed are three scissors modes (blue lines) and three hybridized modes that are combinations of $s$-wave and $d_{x^2-y^2}$- and $d_{z^2}$-basis elements (red line, black line, and green line, respectively).

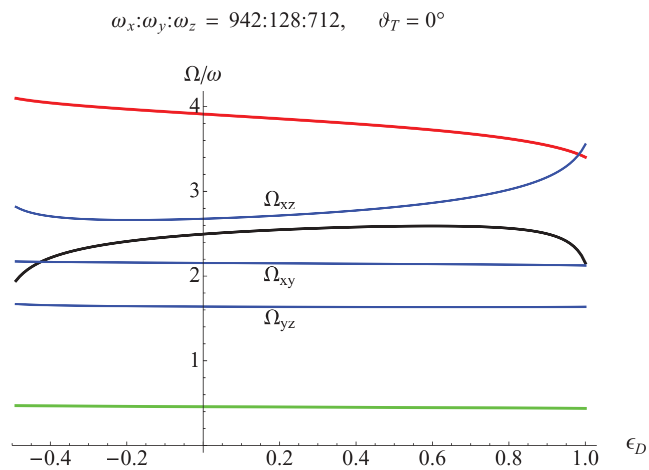


FIG. 10. (Color online) Dependence of eigenfrequencies of small-amplitude collective modes combining isotropic $s$-wave and quadrupolar $d$-wave basis elements vs dipole interaction strength $\varepsilon_D$ for dipolar BEC cloud confined in a harmonic trap with reversed anisotropy ratio $\omega_x{:}\omega_y{:}\omega_z = 942{:}128{:}712$ in the highly symmetric case $\vartheta_T = 0$. Displayed are three scissors modes (blue lines) and three hybridized modes that are combinations of $s$-wave and $d_{x^2-y^2}$- and $d_{z^2}$-basis elements (red line, black line, and green line).

In the highly symmetric case $\vartheta_T = 0$, no coupling of the dilation amplitudes $\widehat{\zeta}_a(\Omega)$ to the off-diagonal elements $a \neq b$ of the tensor $\widehat{\rho}_{ab}$ exists, as is evident from (115). To ease comparison of our results with the results presented in Ref. [9], we also plot in Figs. 11 and 12 the relative change of the collective mode frequencies $\frac{\Omega-\Omega^{(0)}}{\Omega}$ vs $\varepsilon_D$ for the three hybridized modes displayed in Figs. 9 and 10 that couple via the dilatation amplitudes $\widehat{\zeta}_a$ to the time-dependent Thomas-Fermi radii.

It should be pointed out that a purely diagonal shear movement of the dipolar BEC cloud at constant Thomas-Fermi radii, $\widehat{\zeta}_a = 0$, as described by the diagonal elements $\widehat{\eta}^{(1)}_{aa}$ of the tensor $\widehat{\eta}^{(1)}_{ab}$ spanning the (solenoidal) displacement vector field (80), may also excite these hybridized modes

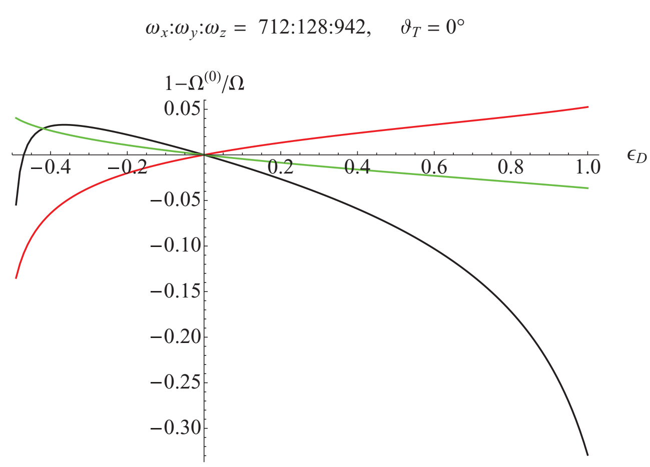


FIG. 11. (Color online) Relative change $\frac{\Omega-\Omega^{(0)}}{\Omega}$ vs $\varepsilon_D$ for the three hybridized collective modes as displayed in Fig. 9 for the highly symmetric case $\vartheta_T = 0$.

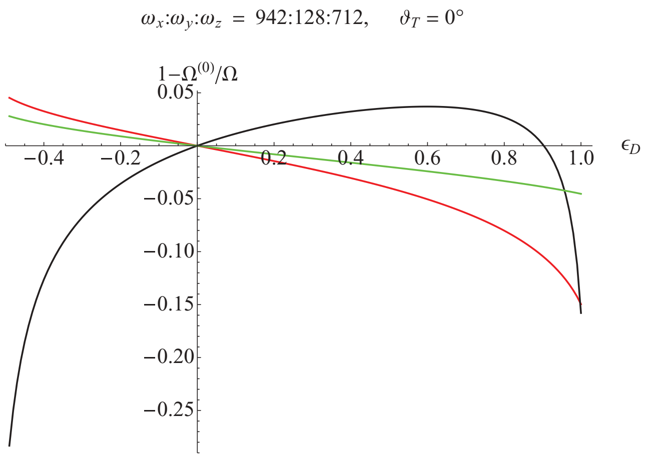


FIG. 12. (Color online) Relative change $\frac{\Omega-\Omega^{(0)}}{\Omega}$ vs $\varepsilon_D$ for the three hybridized collective modes as displayed in Fig. 13 for the highly symmetric case $\vartheta_T = 0$.

coupling to $\widehat{\rho}_{aa}$. This degeneracy is a special property of any quantum degenerate BEC ground state with an ellipsoidal shaped density profile.

### E. Spectrum of low-lying excitations for the case $\vartheta_T \neq 0$

Sudden changes of the trap potential may excite various collective modes of a dipolar BEC cloud. If the polarizing external magnetic field **B** is not in alignment with the principal axis $\mathbf{e}_{z,T}$ of the trap, so $\mathbf{e}_{z,T}$ includes a finite angle $\vartheta_T \neq 0$ with **B** in the $xz$ plane (see Fig. 1), the $s$-wave and $d$-wave symmetry parts of the collective density oscillations combine to a quadruplet and a doublet of modes. It is found from (106) that the modes with mixed $d_{x^2-y^2}$-, $d_{z^2}$-, $d_{xz}$-, and $s$-wave symmetry, consisting of a linear combination of the three diagonal amplitudes $\widehat{\rho}_{xx}$, $\widehat{\rho}_{yy}$, $\widehat{\rho}_{zz}$ and one off-diagonal amplitude $\widehat{\rho}_{xz}$, combine together to a quadruplet (see

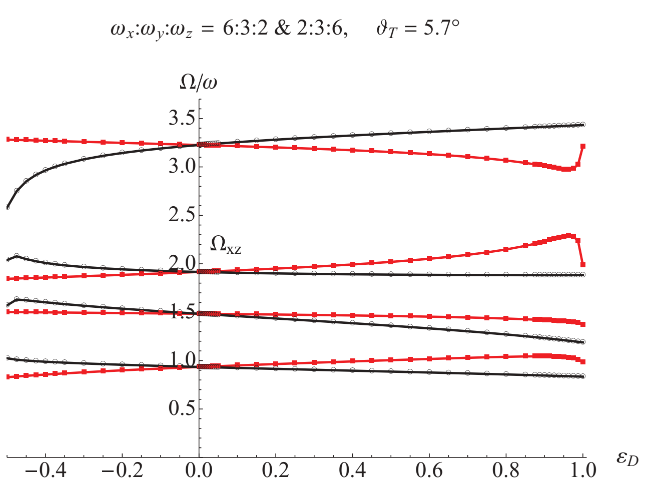


FIG. 13. (Color online) Dependence on dipole interaction strength $\varepsilon_D$ of eigenfrequencies $\Omega$ of small-amplitude density oscillations corresponding to $4 \times 4$ block in (106) when the BEC cloud is confined in a triaxial harmonic anisotropic trap for $\omega_x{:}\omega_y{:}\omega_z =$ 6:3:2 (red line with squares) and $\omega_x{:}\omega_y{:}\omega_z = 2{:}3{:}6$ (black line with circles), choosing a trap orientation angle $\vartheta_T = 5.7°$. All frequencies normalized to geometric mean $\omega = (\omega_x\omega_y\omega_z)^{\frac{1}{3}}$.

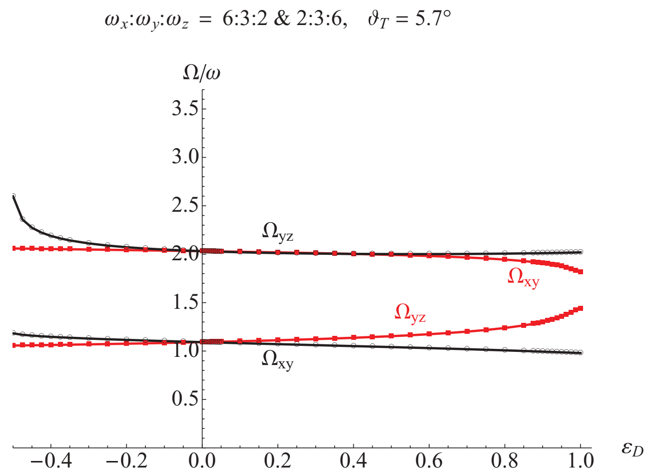


FIG. 14. (Color online) Dependence on dipole interaction strength $\varepsilon_D$ of eigenfrequencies $\Omega$ of small-amplitude density oscillations corresponding to a $2 \times 2$ block in (106) when the BEC cloud is confined in a triaxial harmonic anisotropic trap for $\omega_x{:}\omega_y{:}\omega_z = 6{:}3{:}2$ (red line with squares) and $\omega_x{:}\omega_y{:}\omega_z = 2{:}3{:}6$ (black line with circles), choosing a trap orientation angle $\vartheta_T = 5.7°$. All frequencies are normalized to geometric mean $\omega = (\omega_x\omega_y\omega_z)^{\frac{1}{3}}$.

Fig. 13), and the modes with mixed $d_{xy}$ and $d_{yz}$ symmetry combine together to a doublet of scissors modes (see Fig. 14). From (115) it is evident that for $\varepsilon_D \neq 0$ an infinitesimal rotation around the principal axis $\mathbf{e}_{y,T}$ of a harmonic triaxial trap may then excite via its coupling to the $\widehat{\rho}_{xz}$ components of the eigenvectors all four modes of the mentioned quadruplet of small-amplitude oscillations of the density simultaneously.

Likewise, a rotation around the principal axis $\mathbf{e}_{z,T}$ (or $\mathbf{e}_{x,T}$) of the triaxial harmonic trap may excite, via the coupling to the off-diagonal amplitudes $\widehat{\rho}_{yz}$and $\widehat{\rho}_{xy}$, the mentioned doublet of scissors modes simultaneously. Alternatively, these scissors modes can also be excited by transversal shear movements of the anisotropic harmonic trap, thus creating an excitation of the BEC cloud that may be described by a (solenoidal) displacement vector field (80) that is spanned by the *symmetric* off-diagonal elements of the tensor $\widehat{\eta}_{ab}^{(1)}$.

A sudden change of the curvature of the trap potential, as described by the dilatation amplitudes $\widehat{\zeta}_a$ in (143), excites in the geometry under consideration the modes of the quadruplet but never the scissors modes of the doublet with mixed $d_{xy}$ and $d_{yz}$ symmetry.

The results displayed in Figs. 13 and 14 reveal that a triaxial harmonic trap with trap frequencies $\omega_x = \omega_1$, $\omega_y = \omega_2$, $\omega_z = \omega_3$ (say, $\omega_1 > \omega_2 > \omega_3$) shows a characteristic shift of the eigenfrequencies of these quadruplet- and doublet-collective modes compared to a trap with *reversed* trap frequencies, i.e., a harmonic trap with $\omega_x = \omega_3$, $\omega_y = \omega_2$, and $\omega_z = \omega_1$.

From measurements of these characteristic shifts of the collective mode frequencies of the quadruplet- and doublet-collective modes of a dipolar BEC cloud for two such *mutually reciprocal* triaxial traps the strength of the interaction parameter $\varepsilon_D$ could be determined accurately [21]. Knowing the mass $m^\star$ and the magnetic dipole moment $|\langle\mathbf{M}\rangle|$ of a single atom, one then obtains immediately from (8) the isotropic $s$-wave scattering length of the atoms [9]:

$$a_s = \frac{\mu_0 |\langle \mathbf{M} \rangle|^2}{\frac{12\pi\hbar^2}{m^*}\varepsilon_D}. \tag{144}$$

The experiment suggested here consists in preparing a quantum degenerate spin-polarized dipolar BEC cloud confined in a harmonic trap with triaxial symmetry so the principal axis $\mathbf{e}_{z,T}$ of the trap is first orientated collinear to the spin-polarizing magnetic field $\mathbf{B}$, i.e., at the beginning of the experiment $\vartheta_T = 0 = \vartheta_0$ (see Fig. 1). Then, say, at time $t = 0$, the trap orientation angle $\vartheta_T$ is changed suddenly to a new value by making a rotation around the principal axis $\mathbf{e}_{y,T}$ of the trap by a constant small rotation angle, say, $\vartheta_T = 5.7^\circ$, the value chosen in Figs. 13 and 14. A dipolar BEC cloud excited in this manner will then oscillate, not around the old cloud orientation angle $\vartheta_0 = 0$, but around a new cloud orientation angle $\vartheta_0(\vartheta_T)$, which is via the self-consistency equations (45), (46), and (47) dependent not only on the strength of the dipole interaction parameter $\varepsilon_D$ but also on the chosen trap orientation angle $\vartheta_T$. The principal axis $\mathbf{e}_{z,0}$ of the new equilibrium BEC cloud confined in a harmonic trap with trap orientation angle $\vartheta_T$ then includes with the fixed magnetic field $\mathbf{B}$ a finite angle $\vartheta_0$ that is smaller or larger than $\vartheta_T$, depending on the anisotropy ratio of the trap (see Fig. 2). It follows from what has been said that the eigenfrequencies $\Omega$ of the collective modes of the density fluctuations that can be excited in this manner are functions of $\varepsilon_D$ and the trap orientation angle $\vartheta_T$.

In Figs. 15 and 16 the dependence of the collective mode frequencies of a dipolar BEC cloud on the trap orientation angle $\vartheta_T$ is shown for three values of the interaction strength parameter $\varepsilon_D$.

If a dipolar BEC cloud is confined in a harmonic trap with triaxial symmetry, so the spin polarizing magnetic field $\mathbf{B}$ is orientated in a completely general fashion, i.e., $\mathbf{B}$ its not orientated parallel to any symmetry plane of the trap,

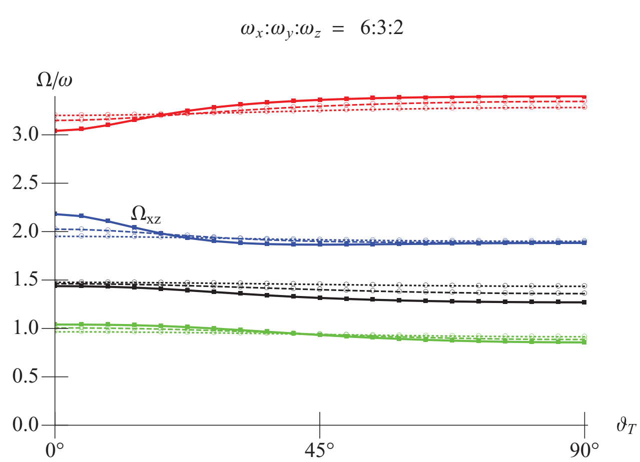


FIG. 15. (Color online) Dependence on trap orientation angle $\vartheta_T$ of eigenfrequencies $\Omega$ of small-amplitude density oscillations corresponding to $4 \times 4$ block in (106) when the BEC cloud is confined in triaxial harmonic anisotropic trap for $\omega_x{:}\omega_y{:}\omega_z = 6{:}3{:}2$. All frequencies normalized to geometric mean $\omega = (\omega_x\omega_y\omega_z)^{\frac{1}{3}}$. The strength of the dipole interaction is $\varepsilon_D = 0.2$ (dotted line), $\varepsilon_D = 0.5$ (dashed line), and $\varepsilon_D = 0.8$ (solid line).

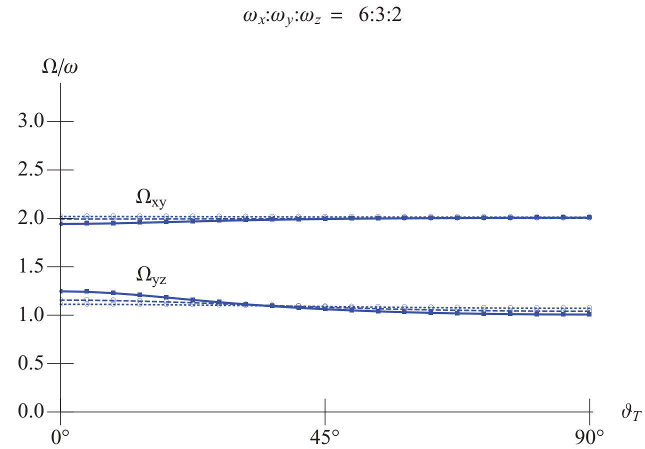


FIG. 16. (Color online) Dependence on trap orientation angle $\vartheta_T$ of eigenfrequencies $\Omega$ of small-amplitude density oscillations corresponding to the $2 \times 2$ block in (106) when the BEC cloud is confined in a triaxial harmonic anisotropic trap for $\omega_x{:}\omega_y{:}\omega_z = 6{:}3{:}2$. All frequencies normalized to geometric mean $\omega = (\omega_x\omega_y\omega_z)^{\frac{1}{3}}$. The strength of the dipole interaction is $\varepsilon_D = 0.2$ (dotted line), $\varepsilon_D = 0.5$ (dashed line), and $\varepsilon_D = 0.8$ (solid line).

the quantum degenerate ground state of the BEC cloud is then characterized by three Euler angles determining the orientation of the ellipsoid $\mathbb{D}_{\rm TF}$ relative to the axes of the trap. We shall present, in a separate publication, a study of such spin-polarized dipolar BEC clouds [16], together with a discussion of the octupolar modes of density oscillations, which can be described by fluctuation amplitudes $\eta^{(2)}_{a;bc}(t)$ associated with a solenoidal vector field with a quadratic spatial variation, i.e., $\eta_a(\mathbf{r},t) = \sum_{b,.c} \eta^{(2)}_{a;bc}(t) r_b r_c$.

## IV. CONCLUSIONS

We have studied the ground state and the low-lying collective modes of a dipolar Bose-Einstein condensate for the case that the external magnetic field is not necessarily oriented parallel to one of the principal axes of the harmonic anisotropic trap. In particular, we have determined the eigenfrequencies of six low-lying collective modes that combine, respectively, to a quadruplet and doublet of atom density oscillations with mixed $s$- and $d$-wave symmetry and obtained analytical expressions for them. We have found the following results: The mode frequencies depend on the dipole interaction parameter in a characteristic way that could be used to measure the $s$-wave scattering length of the atoms accurately. In the special case that the harmonic trap is *spherical* we find the remarkable result that the eigenfrequency of the isotropic breather mode does *not* depend on the dipole interaction strength, even though the shape of the condensate does. Thus, this mode could be used as a reference frequency for the other collective modes that depend on the dipole interaction strength. A rigorous sum-rule argument shows that this feature of the breather mode is a consequence of the scaling property (134) of the interaction potential in a dipolar BEC and the Thomas-Fermi approximation.

*Note added in proof.* Recently an article appeared [24], that addresses the problem to determine the Thomas-Fermi ground state and the low-lying collective excitations of a dipolar BEC, that is confined inside a triaxial harmonic trap for the highly symmetric case, when the polarizing field is orientated strictly parallel to a principal axis of the trap.

## ACKNOWLEDGMENTS

We thank József Fortágh for inspiring discussions. I.S. and T.D. acknowledge support by the DFG (SFB/TRR 21).

## APPENDIX A: INDEX INTEGRALS

Consider the index integrals

$$a,b,c \in \{x,y,z\},$$

$$I_a(\lambda_x,\lambda_y,\lambda_z) = \lambda_x\lambda_y\lambda_z \int_0^\infty \frac{du}{\sqrt{\left(\lambda_x^2+u\right)\left(\lambda_y^2+u\right)\left(\lambda_z^2+u\right)}}\frac{1}{\left(\lambda_a^2+u\right)},$$

$$I_{ab}(\lambda_x,\lambda_y,\lambda_z) = \lambda_x\lambda_y\lambda_z \int_0^\infty \frac{du}{\sqrt{\left(\lambda_x^2+u\right)\left(\lambda_y^2+u\right)\left(\lambda_z^2+u\right)}} \times \frac{1}{\left(\lambda_a^2+u\right)\left(\lambda_b^2+u\right)},$$

$$I_{abc}(\lambda_x,\lambda_y,\lambda_z) = \lambda_x\lambda_y\lambda_z \int_0^\infty \frac{du}{\sqrt{\left(\lambda_x^2+u\right)\left(\lambda_y^2+u\right)\left(\lambda_z^2+u\right)}} \times \frac{1}{\left(\lambda_a^2+u\right)\left(\lambda_b^2+u\right)\left(\lambda_c^2+u\right)}. \tag{A1}$$

These integrals are symmetric under permutations of the indices $a,b,c \in \{x,y,z\}$. It is also evident that

$$\begin{aligned} I_a - I_b &= -\left(\lambda_a^2-\lambda_b^2\right) I_{ab},\\ I_{ac} - I_{bc} &= -\left(\lambda_a^2-\lambda_b^2\right) I_{abc}. \end{aligned} \tag{A2}$$

Also index integrals $I_{ab}$ and $I_{abc}$ are connected by a derivative operation:

$$\left(\frac{1}{\lambda_c} - \frac{\partial}{\partial\lambda_c}\right) I_{ab} = (1+2\delta_{ac}+2\delta_{bc})\,\lambda_c I_{abc}. \tag{A3}$$

Let us note the identity

$$\left(-2\frac{d}{du}\right)\left[\frac{1}{\sqrt{\left(\lambda_x^2+u\right)\left(\lambda_y^2+u\right)\left(\lambda_z^2+u\right)}}\right] = \frac{1}{\sqrt{\left(\lambda_x^2+u\right)\left(\lambda_y^2+u\right)\left(\lambda_z^2+u\right)}} \sum_{a\in\{x,y,z\}} \frac{1}{\lambda_a^2+u}. \tag{A4}$$

Likewise,

$$\left(-2\frac{d}{du}\right)\left[\frac{1}{\sqrt{\left(\lambda_x^2+u\right)\left(\lambda_y^2+u\right)\left(\lambda_z^2+u\right)}}\frac{1}{\lambda_b^2+u}\right] = \frac{1}{\sqrt{\left(\lambda_x^2+u\right)\left(\lambda_y^2+u\right)\left(\lambda_z^2+u\right)}}\frac{1}{\lambda_b^2+u} \times \left[\frac{2}{\lambda_b^2+u} + \sum_{a\in\{x,y,z\}} \frac{1}{\lambda_a^2+u}\right] \tag{A5}$$

and

$$\left(-2\frac{d}{du}\right)\left[\frac{1}{\sqrt{\left(\lambda_x^2+u\right)\left(\lambda_y^2+u\right)\left(\lambda_z^2+u\right)}}\frac{1}{\lambda_b^2+u}\frac{1}{\lambda_c^2+u}\right] = \frac{1}{\sqrt{\left(\lambda_x^2+u\right)\left(\lambda_y^2+u\right)\left(\lambda_z^2+u\right)}}\frac{1}{\lambda_b^2+u}\frac{1}{\lambda_c^2+u} \times \left[\frac{2}{\lambda_b^2+u} + \frac{2}{\lambda_c^2+u} + \sum_{a\in\{x,y,z\}} \frac{1}{\lambda_a^2+u}\right]. \tag{A6}$$

On integration with respect to the variable $u$ from 0 to $\infty$ there follow now several useful identities:

$$\begin{aligned} 2 &= \sum_{a\in\{x,y,z\}} I_a,\\ \frac{2}{\lambda_b^2} &= 2I_{bb} + \sum_{a\in\{x,y,z\}} I_{ba},\\ \frac{2}{\lambda_b^2\lambda_c^2} &= 2I_{bbc} + 2I_{bcc} + \sum_{a\in\{x,y,z\}} I_{bca}, \end{aligned} \tag{A7}$$

Using these relations, various useful algebraic connections between the integrals $I_a$ and $I_{ab}$, and between $I_{ab}$ and $I_{abc}$, become evident [11]:

$$\begin{gathered} a,b,c \in \{x,y,z\},\\ a \neq b \neq c,\\ 3I_{aa}\lambda_a^2 + I_{ab}\lambda_b^2 + I_{ac}\lambda_c^2 = 3I_a,\\ 5I_{aaa}\lambda_a^2 + I_{aab}\lambda_b^2 + I_{aac}\lambda_c^2 = 5I_{aa},\\ 3I_{aab}\lambda_a^2 + 3I_{abb}\lambda_b^2 + I_{abc}\lambda_c^2 = 5I_{ab}. \end{gathered} \tag{A8}$$

Making the substitution

$$u \to u = \Lambda^2 u', \tag{A9}$$

we obtain useful scaling relations

$$\begin{aligned} I_a(\lambda_x,\lambda_y,\lambda_z) &= I_a\left(\frac{\lambda_x}{\Lambda},\frac{\lambda_y}{\Lambda},\frac{\lambda_z}{\Lambda}\right) \equiv \overline{I}_a,\\ I_{ab}(\lambda_x,\lambda_y,\lambda_z) &= \frac{1}{\Lambda^2} I_{ab}\left(\frac{\lambda_x}{\Lambda},\frac{\lambda_y}{\Lambda},\frac{\lambda_z}{\Lambda}\right) \equiv \frac{1}{\Lambda^2}\overline{I}_{ab},\\ I_{abc}(\lambda_x,\lambda_y,\lambda_z) &= \frac{1}{\Lambda^4} I_{abc}\left(\frac{\lambda_x}{\Lambda},\frac{\lambda_y}{\Lambda},\frac{\lambda_z}{\Lambda}\right) \equiv \frac{1}{\Lambda^4}\overline{I}_{abc}. \end{aligned} \tag{A10}$$

In our calculations we find it convenient to choose $\Lambda = \lambda_z > 0$.

The task to calculate double-index integrals $I_{ab}$ can be reduced to calculating simpler single-index integrals $I_a$. This is enabled by using

$$\overline{I}_{zz} = \frac{2-\overline{I}_{zx}-\overline{I}_{zy}}{3}, \tag{A11}$$

an immediate consequence of (A7). Provided $\lambda_a \neq \lambda_z$, the integrals $\overline{I}_{za}$ can be reduced to calculating the simpler integrals $\overline{I}_z$ and $\overline{I}_a$ using the identity

$$a \in \{x,y\}, \quad \overline{I}_{za} = -\frac{\overline{I}_z - \overline{I}_a}{1-\frac{\lambda_a^2}{\lambda_z^2}}. \tag{A12}$$

So for $\lambda_a \neq \lambda_z$ all double-index integrals $\overline{I}_{za}$ can be reduced to single-index integrals $\overline{I}_a$. Carlson [22] has provided an elegant and efficient algorithm based on the well-known method of the arithmetic-geometric mean to calculate the single-index integral $\overline{I}_a$ directly, a method we highly recommend because of its accuracy and speed [23].

For $\lambda_a = \lambda_z$ the right-hand side becomes formally undefined. However, in this case we may calculate the integrals $\overline{I}_{zx}$ and $\overline{I}_{zy}$ in closed form:

$$\lim_{\lambda_a\to\lambda_z} \overline{I}_{za} = \lim_{\lambda_a\to\lambda_z} \frac{\lambda_x}{\lambda_z}\frac{\lambda_y}{\lambda_z}\int_0^\infty \frac{du}{\sqrt{\left(\frac{\lambda_x^2}{\lambda_z^2}+u\right)\left(\frac{\lambda_y^2}{\lambda_z^2}+u\right)(1+u)}} \times \frac{1}{(1+u)\left(\frac{\lambda_a^2}{\lambda_z^2}+u\right)},$$

$$\lim_{\lambda_x\to\lambda_z} \overline{I}_{zx} = \frac{\lambda_y}{\lambda_z}\int_0^\infty \frac{du}{\sqrt{\frac{\lambda_y^2}{\lambda_z^2}+u}}\frac{1}{(1+u)^3} \equiv I\left(\frac{\lambda_y}{\lambda_z}\right),$$

$$\lim_{\lambda_y\to\lambda_z} \overline{I}_{zy} = \frac{\lambda_x}{\lambda_z}\int_0^\infty \frac{du}{\sqrt{\frac{\lambda_x^2}{\lambda_z^2}+u}}\frac{1}{(1+u)^3} \equiv I\left(\frac{\lambda_x}{\lambda_z}\right),$$

$$I(q) = q\int_0^\infty \frac{du}{\sqrt{q^2+u}}\frac{1}{(1+u)^3} = \frac{q}{4(q^2-1)^2}\left(2q^3-5q+3\frac{\operatorname{arccosh}(q)}{\sqrt{q^2-1}}\right). \tag{A13}$$

In the isotropic case $\lambda_z = \lambda_x = \lambda_y$

$$\lim_{\lambda_x\to\lambda_z}\lim_{\lambda_y\to\lambda_z} \overline{I}_{zy} = \lim_{\lambda_y\to\lambda_z}\lim_{\lambda_x\to\lambda_z} \overline{I}_{zx} = I(1) = \frac{2}{5}. \tag{A14}$$

## APPENDIX B: SUM RULE

The sum rule

$$\sum_a w_{aa}(t) = 5w_{00}(t) \tag{B1}$$

follows directly from the defining equations (98) and the properties of the triple-index integrals:

$$\begin{aligned}\sum_a w_{aa}(t) = \Bigg\{&\frac{3}{2}\varepsilon_D \times \big[\lambda_x^2[\cos^2(\vartheta_0)(3I_{xxz}+I_{xyz}+3I_{xzz})+3\sin^2(\vartheta_0)(5I_{xxx}+I_{xxy}+I_{xxz})]\rho_{xx}(t)\\ &+\lambda_y^2[\cos^2(\vartheta_0)(I_{xyz}+3I_{yyz}+3I_{yzz})+\sin^2(\vartheta_0)(3I_{xxy}+3I_{xyy}+I_{xyz})]\rho_{yy}(t)\\ &+\lambda_z^2[3\cos^2(\vartheta_0)(I_{xzz}+I_{yzz}+5I_{zzz})+\sin^2(\vartheta_0)(3I_{xxz}+I_{xyz}+3I_{xzz})]\rho_{zz}(t)\\ &+\sin(2\vartheta_0)\lambda_z\lambda_x(3I_{xxz}+I_{xyz}+3I_{xzz})\rho_{xz}(t)\big]+5(1-\varepsilon_D)\left[\frac{1}{\lambda_x^2}\rho_{xx}(t)+\frac{1}{\lambda_y^2}\rho_{yy}(t)+\frac{1}{\lambda_z^2}\rho_{zz}(t)\right]\\ &+\left[5\frac{1-\varepsilon_D}{2}\left(\frac{1}{\lambda_x^2}+\frac{1}{\lambda_y^2}+\frac{1}{\lambda_z^2}\right)+\frac{9\varepsilon_D}{2}\left(\frac{\cos^2(\vartheta_0)}{\lambda_z^2}+\frac{\sin^2(\vartheta_0)}{\lambda_x^2}\right)\right]\rho_{00}(t)\\ &+9\varepsilon_D\left[\frac{\sin^2(\vartheta_0)}{\lambda_x^2}\rho_{xx}(t)+\frac{\cos^2(\vartheta_0)}{\lambda_z^2}\rho_{zz}(t)+\frac{\sin(2\vartheta_0)}{2\lambda_x\lambda_z}\rho_{xz}(t)\right]\Bigg\}.\end{aligned} \tag{B2}$$

There holds the following identity for the index integrals $I_{abc}$:

$$a,b \in \{x,y,z\}, \quad 2I_{aab}+2I_{abb}+I_{abx}+I_{aby}+I_{abz} = \frac{2}{\lambda_a^2\lambda_b^2}. \tag{B3}$$

Taking into account that the index integrals $I_{abc}$ are invariant under permutations of their indices $a,b,c \in \{x,y,z\}$, it follows for the linear combinations encountered in (B2) that

$$3I_{xxz}+I_{xyz}+3I_{xzz} = 2I_{xxz}+2I_{xzz}+I_{xzx}+I_{xzy}+I_{xzz} = \frac{2}{\lambda_x^2\lambda_z^2},$$

$$5I_{xxx}+I_{xxy}+I_{xxz} = 2I_{xxx}+2I_{xxx}+I_{xxx}+I_{xxy}+I_{xxz} = \frac{2}{\lambda_x^2\lambda_x^2} = \frac{2}{\lambda_x^4},$$

$$I_{xyz}+3I_{yyz}+3I_{yzz} = 2I_{yyz}+2I_{yzz}+I_{yzx}+I_{yzy}+I_{yzz} = \frac{2}{\lambda_y^2\lambda_z^2},$$

$$3I_{xxy}+3I_{xyy}+I_{xyz} = 2I_{xxy}+2I_{xyy}+I_{xyx}+I_{xyy}+I_{xyz} = \frac{2}{\lambda_x^2\lambda_y^2},$$

$$I_{xzz}+I_{yzz}+5I_{zzz} = 2I_{zzz}+2I_{zzz}+I_{zzx}+I_{zzy}+I_{zzz} = \frac{2}{\lambda_z^2\lambda_z^2} = \frac{2}{\lambda_z^4}.$$

Making use of these identities, and taking into account (101), we indeed see that

$$\begin{aligned}\sum_{a\in\{x,y,z\}} w_{aa}(t) &= \Bigg\{3\varepsilon_D\Bigg(\left[\cos^2(\vartheta_0)\frac{1}{\lambda_z^2}+3\sin^2(\vartheta_0)\frac{1}{\lambda_x^2}\right]\rho_{xx}(t)+\left[\cos^2(\vartheta_0)\frac{1}{\lambda_z^2}+\sin^2(\vartheta_0)\frac{1}{\lambda_x^2}\right]\rho_{yy}(t)\\
&\quad+\left[3\cos^2(\vartheta_0)\frac{1}{\lambda_z^2}+\sin^2(\vartheta_0)\frac{1}{\lambda_x^2}\right]\rho_{zz}(t)+\sin(2\vartheta_0)\,\frac{1}{\lambda_x\lambda_z}\rho_{xz}(t)\Bigg)\\
&\quad+5(1-\varepsilon_D)\left[\frac{1}{\lambda_x^2}\rho_{xx}(t)+\frac{1}{\lambda_y^2}\rho_{yy}(t)+\frac{1}{\lambda_z^2}\rho_{zz}(t)\right]\\
&\quad+\left[5\frac{1-\varepsilon_D}{2}\left(\frac{1}{\lambda_x^2}+\frac{1}{\lambda_y^2}+\frac{1}{\lambda_z^2}\right)+\frac{9\varepsilon_D}{2}\left(\frac{\cos^2(\vartheta_0)}{\lambda_z^2}+\frac{\sin^2(\vartheta_0)}{\lambda_x^2}\right)\right]\rho_{00}(t)\\
&\quad+9\varepsilon_D\left[\frac{\sin^2(\vartheta_0)}{\lambda_x^2}\rho_{xx}(t)+\frac{\cos^2(\vartheta_0)}{\lambda_z^2}\rho_{zz}(t)+\frac{\sin(2\vartheta_0)}{2\lambda_x\lambda_z}\rho_{xz}(t)\right]\Bigg\}\\
&= \Bigg\{3\varepsilon_D\left[\cos^2(\vartheta_0)\frac{1}{\lambda_z^2}+\sin^2(\vartheta_0)\frac{1}{\lambda_x^2}\right]\left[\rho_{xx}(t)+\rho_{yy}(t)+\rho_{zz}(t)\right]\\
&\quad+5(1-\varepsilon_D)\left[\frac{1}{\lambda_x^2}\rho_{xx}(t)+\frac{1}{\lambda_y^2}\rho_{yy}(t)+\frac{1}{\lambda_z^2}\rho_{zz}(t)\right]\\
&\quad+\left[5\frac{1-\varepsilon_D}{2}\left(\frac{1}{\lambda_x^2}+\frac{1}{\lambda_y^2}+\frac{1}{\lambda_z^2}\right)+\frac{9\varepsilon_D}{2}\left(\frac{\cos^2(\vartheta_0)}{\lambda_z^2}+\frac{\sin^2(\vartheta_0)}{\lambda_x^2}\right)\right]\rho_{00}(t)\\
&\quad+3\varepsilon_D\,(3+2)\left[\frac{\sin^2(\vartheta_0)}{\lambda_x^2}\rho_{xx}(t)+\frac{\cos^2(\vartheta_0)}{\lambda_z^2}\rho_{zz}(t)+\frac{\sin(2\vartheta_0)}{2\lambda_x\lambda_z}\rho_{xz}(t)\right]\Bigg\}\\
&= 5\Bigg\{(1-\varepsilon_D)\left[\frac{1}{\lambda_x^2}\rho_{xx}(t)+\frac{1}{\lambda_y^2}\rho_{yy}(t)+\frac{1}{\lambda_z^2}\rho_{zz}(t)\right]+3\varepsilon_D\left[\frac{\cos^2(\vartheta_0)}{\lambda_z^2}\rho_{zz}(t)+\frac{\sin^2(\vartheta_0)}{\lambda_x^2}\rho_{xx}(t)+\frac{\sin(2\vartheta_0)}{2\lambda_x\lambda_z}\rho_{xz}(t)\right]\\
&\quad+\left[\frac{1-\varepsilon_D}{2}\left(\frac{1}{\lambda_x^2}+\frac{1}{\lambda_y^2}+\frac{1}{\lambda_z^2}\right)+\frac{3\varepsilon_D}{2}\left(\frac{\cos^2(\vartheta_0)}{\lambda_z^2}+\frac{\sin^2(\vartheta_0)}{\lambda_x^2}\right)\right]\rho_{00}(t)\Bigg\}\\
&= 5w_{00}(t).\end{aligned}\tag{B4}$$

## APPENDIX C: EXPLICIT EXPRESSIONS FOR $G_{ab}(t)-F_{ab}(t)$ AND MATRIX ELEMENTS $C_{ab,cd}$

We collect here explicit expressions for the linear combinations $G_{ab}(t)-F_{ab}(t)$ that occur in (98),

$$\begin{aligned}G_{xx}(t)-F_{xx}(t) &= \frac{1}{\lambda_x^2}\big\{3\lambda_x^2[\cos^2(\vartheta_0)I_{xxz}+5\sin^2(\vartheta_0)I_{xxx}]\rho_{xx}(t)+\lambda_y^2[\cos^2(\vartheta_0)I_{xyz}+3\sin^2(\vartheta_0)I_{xxy}]\rho_{yy}(t)\\
&\quad+3\lambda_z^2[\cos^2(\vartheta_0)I_{xzz}+\sin^2(\vartheta_0)I_{xxz}]\rho_{zz}(t)+3\sin(2\vartheta_0)\,I_{xxz}\lambda_x\lambda_z\rho_{xz}(t)\big\},\\
G_{yy}(t)-F_{yy}(t) &= \frac{1}{\lambda_y^2}\big\{\lambda_x^2[\cos^2(\vartheta_0)I_{xyz}+3\sin^2(\vartheta_0)I_{xxy}]\rho_{xx}(t)+3\lambda_y^2[\cos^2(\vartheta_0)I_{yyz}+\sin^2(\vartheta_0)I_{xyy}]\rho_{yy}(t)\\
&\quad+\lambda_z^2[3\cos^2(\vartheta_0)I_{yzz}+\sin^2(\vartheta_0)I_{xyz}]\rho_{zz}(t)+\sin(2\vartheta_0)\,I_{xyz}\cdot\lambda_x\lambda_z\rho_{xz}(t)\big\},\\
G_{zz}(t)-F_{zz}(t) &= \frac{1}{\lambda_z^2}\big\{3\lambda_x^2[\cos^2(\vartheta_0)I_{xzz}+\sin^2(\vartheta_0)I_{xxz}]\rho_{xx}(t)+\lambda_y^2[3\cos^2(\vartheta_0)I_{yzz}+\sin^2(\vartheta_0)I_{xyz}]\rho_{yy}(t)\\
&\quad+3\lambda_z^2[5\cos^2(\vartheta_0)I_{zzz}+\sin^2(\vartheta_0)I_{xzz}]\rho_{zz}(t)+3\sin(2\vartheta_0)\,I_{xzz}\lambda_x\lambda_z\rho_{xz}(t)\big\},\end{aligned}\tag{C1}$$

and also in (99),

$$G_{xz}(t)-F_{xz}(t)=\Bigg\{3\left(\frac{1}{\lambda_x^2}+\frac{1}{\lambda_z^2}\right)\lambda_x\lambda_z\left[\cos^2(\vartheta_0)I_{xzz}+\sin^2(\vartheta_0)I_{xxz}\right]\rho_{xz}(t)$$
$$+\sin(2\vartheta_0)\left[3\left(1+\frac{\lambda_x^2}{\lambda_z^2}\right)I_{xxz}\rho_{xx}(t)+\left(\frac{\lambda_y^2}{\lambda_x^2}+\frac{\lambda_y^2}{\lambda_z^2}\right)I_{xyz}\rho_{yy}(t)+3\left(\frac{\lambda_z^2}{\lambda_x^2}+1\right)I_{xzz}\rho_{zz}(t)\right]\Bigg\},$$
$$G_{yz}(t)-F_{yz}(t)=\left(\frac{1}{\lambda_y^2}+\frac{1}{\lambda_z^2}\right)[\sin(2\vartheta_0)\,\lambda_x\lambda_yI_{xyz}\rho_{xy}(t)+\lambda_y\lambda_z[3\cos^2(\vartheta_0)I_{yzz}+\sin^2(\vartheta_0)I_{xyz}]\rho_{yz}(t)],$$
$$G_{xy}(t)-F_{xy}(t)=\left(\frac{1}{\lambda_x^2}+\frac{1}{\lambda_y^2}\right)[\lambda_x\lambda_y[\cos^2(\vartheta_0)I_{xyz}+3\sin^2(\vartheta_0)I_{xxy}]\rho_{xy}(t)+\lambda_y\lambda_z\sin(2\vartheta_0)\,I_{xyz}\rho_{yz}(t)].$$

The matrix elements $C_{ab,cd}$ occurring in the eigenvalue problem (106) are explicitly given by

$$\frac{2n_0g^{(s)}}{m^\star}C_{xx,xx}=\omega_y^2\frac{\lambda_y^2}{\lambda_x^2}\frac{3(1-\varepsilon_D)+\frac{9}{2}\varepsilon_D\frac{\lambda_x^4}{\lambda_z^4}[\cos^2(\vartheta_0)\overline{I}_{xxz}+5\sin^2(\vartheta_0)\overline{I}_{xxx}]}{1-\varepsilon_D+\frac{3\varepsilon_D}{2}\frac{\lambda_y^2}{\lambda_z^2}[\cos^2(\vartheta_0)\overline{I}_{zy}+\sin^2(\vartheta_0)\overline{I}_{xy}]},$$
$$\frac{2n_0g^{(s)}}{m^\star}C_{xx,yy}=\omega_y^2\frac{\lambda_y^2}{\lambda_x^2}\frac{(1-\varepsilon_D)+\frac{3}{2}\varepsilon_D\frac{\lambda_x^2}{\lambda_z^2}\frac{\lambda_y^2}{\lambda_z^2}[\cos^2(\vartheta_0)\overline{I}_{xyz}+3\sin^2(\vartheta_0)\overline{I}_{xxy}]}{1-\varepsilon_D+\frac{3\varepsilon_D}{2}\frac{\lambda_y^2}{\lambda_z^2}[\cos^2(\vartheta_0)\overline{I}_{zy}+\sin^2(\vartheta_0)\overline{I}_{xy}]},$$
$$\frac{2n_0g^{(s)}}{m^\star}C_{xx,zz}=\omega_y^2\frac{\lambda_y^2}{\lambda_x^2}\frac{(1-\varepsilon_D)+\frac{9}{2}\varepsilon_D\frac{\lambda_x^2}{\lambda_z^2}[\cos^2(\vartheta_0)\overline{I}_{xzz}+\sin^2(\vartheta_0)\overline{I}_{xxz}]}{1-\varepsilon_D+\frac{3\varepsilon_D}{2}\frac{\lambda_y^2}{\lambda_z^2}[\cos^2(\vartheta_0)\overline{I}_{zy}+\sin^2(\vartheta_0)\overline{I}_{xy}]},\tag{C2}$$
$$\frac{2n_0g^{(s)}}{m^\star}C_{xx,xz}=\omega_y^2\frac{\frac{9}{2}\varepsilon_D\sin(2\vartheta_0)\frac{\lambda_x}{\lambda_z}\frac{\lambda_y^2}{\lambda_z^2}\overline{I}_{xxz}}{1-\varepsilon_D+\frac{3\varepsilon_D}{2}\frac{\lambda_y^2}{\lambda_z^2}[\cos^2(\vartheta_0)\overline{I}_{zy}+\sin^2(\vartheta_0)\overline{I}_{xy}]},$$

$$\frac{2n_0g^{(s)}}{m^\star}C_{yy,xx}=\omega_y^2\frac{(1-\varepsilon_D)+\frac{3}{2}\varepsilon_D\frac{\lambda_x^2}{\lambda_z^2}\frac{\lambda_y^2}{\lambda_z^2}[\cos^2(\vartheta_0)\overline{I}_{xyz}+3\sin^2(\vartheta_0)\overline{I}_{xxy}]}{1-\varepsilon_D+\frac{3\varepsilon_D}{2}\frac{\lambda_y^2}{\lambda_z^2}[\cos^2(\vartheta_0)\overline{I}_{zy}+\sin^2(\vartheta_0)\overline{I}_{xy}]},$$
$$\frac{2n_0g^{(s)}}{m^\star}C_{yy,yy}=\omega_y^2\frac{3(1-\varepsilon_D)+\frac{9}{2}\varepsilon_D\frac{\lambda_y^4}{\lambda_z^4}[\cos^2(\vartheta_0)\overline{I}_{yyz}+\sin^2(\vartheta_0)\overline{I}_{xyy}]}{1-\varepsilon_D+\frac{3\varepsilon_D}{2}\frac{\lambda_y^2}{\lambda_z^2}[\cos^2(\vartheta_0)\overline{I}_{zy}+\sin^2(\vartheta_0)\overline{I}_{xy}]},$$
$$\frac{2n_0g^{(s)}}{m^\star}C_{yy,zz}=\omega_y^2\frac{(1-\varepsilon_D)+\frac{3}{2}\varepsilon_D\frac{\lambda_y^2}{\lambda_z^2}[3\cos^2(\vartheta_0)\overline{I}_{yzz}+\sin^2(\vartheta_0)\overline{I}_{xyz}]}{1-\varepsilon_D+\frac{3\varepsilon_D}{2}\frac{\lambda_y^2}{\lambda_z^2}[\cos^2(\vartheta_0)\overline{I}_{zy}+\sin^2(\vartheta_0)\overline{I}_{xy}]},\tag{C3}$$
$$\frac{2n_0g^{(s)}}{m^\star}C_{yy,xz}=\omega_y^2\frac{\frac{3}{2}\varepsilon_D\sin(2\vartheta_0)\frac{\lambda_x}{\lambda_z}\frac{\lambda_y^2}{\lambda_z^2}\overline{I}_{xyz}}{1-\varepsilon_D+\frac{3\varepsilon_D}{2}\frac{\lambda_y^2}{\lambda_z^2}[\cos^2(\vartheta_0)\overline{I}_{zy}+\sin^2(\vartheta_0)\overline{I}_{xy}]},$$

$$\frac{2n_0g^{(s)}}{m^\star}C_{zz,xx}=\omega_y^2\frac{\lambda_y^2}{\lambda_z^2}\frac{(1-\varepsilon_D)+\frac{9}{2}\varepsilon_D\frac{\lambda_x^2}{\lambda_z^2}[\cos^2(\vartheta_0)\overline{I}_{xzz}+\sin^2(\vartheta_0)\overline{I}_{xxz}]}{1-\varepsilon_D+\frac{3\varepsilon_D}{2}\frac{\lambda_y^2}{\lambda_z^2}[\cos^2(\vartheta_0)\overline{I}_{zy}+\sin^2(\vartheta_0)\overline{I}_{xy}]},$$
$$\frac{2n_0g^{(s)}}{m^\star}C_{zz,yy}=\omega_y^2\frac{\lambda_y^2}{\lambda_z^2}\frac{(1-\varepsilon_D)+\frac{3}{2}\varepsilon_D\frac{\lambda_y^2}{\lambda_z^2}[3\cos^2(\vartheta_0)\overline{I}_{yzz}+\sin^2(\vartheta_0)\overline{I}_{xyz}]}{1-\varepsilon_D+\frac{3\varepsilon_D}{2}\frac{\lambda_y^2}{\lambda_z^2}[\cos^2(\vartheta_0)\overline{I}_{zy}+\sin^2(\vartheta_0)\overline{I}_{xy}]},$$
$$\frac{2n_0g^{(s)}}{m^\star}C_{zz,zz}=\omega_y^2\frac{\lambda_y^2}{\lambda_z^2}\frac{3(1-\varepsilon_D)+\frac{9}{2}\varepsilon_D[5\cos^2(\vartheta_0)\overline{I}_{zzz}+\sin^2(\vartheta_0)\overline{I}_{xzz}]}{1-\varepsilon_D+\frac{3\varepsilon_D}{2}\frac{\lambda_y^2}{\lambda_z^2}[\cos^2(\vartheta_0)\overline{I}_{zy}+\sin^2(\vartheta_0)\overline{I}_{xy}]},\tag{C4}$$

$$\frac{2n_0g^{(s)}}{m^\star}C_{zz,xz}=\omega_y^2\frac{\frac{9}{2}\varepsilon_D\sin(2\vartheta_0)\frac{\lambda_x}{\lambda_z}\frac{\lambda_y^2}{\lambda_z^2}\overline{I}_{xzz}}{1-\varepsilon_D+\frac{3\varepsilon_D}{2}\frac{\lambda_y^2}{\lambda_z^2}[\cos^2(\vartheta_0)\overline{I}_{zy}+\sin^2(\vartheta_0)\overline{I}_{xy}]},$$

$$\frac{2n_0g^{(s)}}{m^\star}C_{xz,xx}=\omega_y^2\left(1+\frac{\lambda_x^2}{\lambda_z^2}\right)\frac{\frac{9}{2}\varepsilon_D\sin(2\vartheta_0)\frac{\lambda_x}{\lambda_z}\frac{\lambda_y^2}{\lambda_z^2}\overline{I}_{xxz}}{1-\varepsilon_D+\frac{3\varepsilon_D}{2}\frac{\lambda_y^2}{\lambda_z^2}[\cos^2(\vartheta_0)\overline{I}_{zy}+\sin^2(\vartheta_0)\overline{I}_{xy}]},$$

$$\frac{2n_0g^{(s)}}{m^\star}C_{xz,yy}=\omega_y^2\left(\frac{\lambda_y^2}{\lambda_x^2}+\frac{\lambda_y^2}{\lambda_z^2}\right)\frac{\frac{3}{2}\varepsilon_D\sin(2\vartheta_0)\frac{\lambda_x}{\lambda_z}\frac{\lambda_y^2}{\lambda_z^2}\overline{I}_{xyz}}{1-\varepsilon_D+\frac{3\varepsilon_D}{2}\frac{\lambda_y^2}{\lambda_z^2}[\cos^2(\vartheta_0)\overline{I}_{zy}+\sin^2(\vartheta_0)\overline{I}_{xy}]},\tag{C5}$$

$$\frac{2n_0g^{(s)}}{m^\star}C_{xz,zz}=\omega_y^2\left(1+\frac{\lambda_z^2}{\lambda_x^2}\right)\frac{\frac{9}{2}\varepsilon_D\sin(2\vartheta_0)\frac{\lambda_x}{\lambda_z}\frac{\lambda_y^2}{\lambda_z^2}\overline{I}_{xzz}}{1-\varepsilon_D+\frac{3\varepsilon_D}{2}\frac{\lambda_y^2}{\lambda_z^2}[\cos^2(\vartheta_0)\overline{I}_{zy}+\sin^2(\vartheta_0)\overline{I}_{xy}]},$$

$$\frac{2n_0g^{(s)}}{m^\star}C_{xz,xz}=\omega_y^2\left(\frac{\lambda_y^2}{\lambda_x^2}+\frac{\lambda_y^2}{\lambda_z^2}\right)\frac{(1-\varepsilon_D)+\frac{9}{2}\varepsilon_D\frac{\lambda_x^2}{\lambda_z^2}[\cos^2(\vartheta_0)\overline{I}_{xzz}+\sin^2(\vartheta_0)\overline{I}_{xxz}]}{1-\varepsilon_D+\frac{3\varepsilon_D}{2}\frac{\lambda_y^2}{\lambda_z^2}[\cos^2(\vartheta_0)\overline{I}_{zy}+\sin^2(\vartheta_0)\overline{I}_{xy}]},$$

$$\frac{2n_0g^{(s)}}{m^\star}C_{yz,yz}=\omega_y^2\left(1+\frac{\lambda_y^2}{\lambda_z^2}\right)\frac{(1-\varepsilon_D)+\frac{3}{2}\varepsilon_D\frac{\lambda_y^2}{\lambda_z^2}[3\cos^2(\vartheta_0)\overline{I}_{yzz}+\sin^2(\vartheta_0)\overline{I}_{xyz}]}{1-\varepsilon_D+\frac{3\varepsilon_D}{2}\frac{\lambda_y^2}{\lambda_z^2}[\cos^2(\vartheta_0)\overline{I}_{zy}+\sin^2(\vartheta_0)\overline{I}_{xy}]},\tag{C6}$$

$$\frac{2n_0g^{(s)}}{m^\star}C_{yz,xy}=\omega_y^2\left(1+\frac{\lambda_y^2}{\lambda_z^2}\right)\frac{\frac{3}{2}\varepsilon_D\sin(2\vartheta_0)\frac{\lambda_x}{\lambda_z}\frac{\lambda_y^2}{\lambda_z^2}\overline{I}_{xyz}}{1-\varepsilon_D+\frac{3\varepsilon_D}{2}\frac{\lambda_y^2}{\lambda_z^2}[\cos^2(\vartheta_0)\overline{I}_{zy}+\sin^2(\vartheta_0)\overline{I}_{xy}]},$$

$$\frac{2n_0g^{(s)}}{m^\star}C_{xy,yz}=\omega_y^2\left(1+\frac{\lambda_y^2}{\lambda_x^2}\right)\frac{\frac{3}{2}\varepsilon_D\sin(2\vartheta_0)\frac{\lambda_x}{\lambda_z}\frac{\lambda_y^2}{\lambda_z^2}\overline{I}_{xyz}}{1-\varepsilon_D+\frac{3\varepsilon_D}{2}\frac{\lambda_y^2}{\lambda_z^2}[\cos^2(\vartheta_0)\overline{I}_{zy}+\sin^2(\vartheta_0)\overline{I}_{xy}]},\tag{C7}$$

$$\frac{2n_0g^{(s)}}{m^\star}C_{xy,xy}=\omega_y^2\left(1+\frac{\lambda_y^2}{\lambda_x^2}\right)\frac{(1-\varepsilon_D)+\frac{3}{2}\varepsilon_D\frac{\lambda_x^2}{\lambda_z^2}\frac{\lambda_y^2}{\lambda_z^2}[\cos^2(\vartheta_0)\overline{I}_{xyz}+3\sin^2(\vartheta_0)\overline{I}_{xxy}]}{1-\varepsilon_D+\frac{3\varepsilon_D}{2}\frac{\lambda_y^2}{\lambda_z^2}[\cos^2(\vartheta_0)\overline{I}_{zy}+\sin^2(\vartheta_0)\overline{I}_{xy}]}.$$

Here, the quantities $\overline{I}_{ab}$ and $\overline{I}_{abc}$ denote (scaled) double- and triple-index integrals, as explained in (A10).

## APPENDIX D: COUPLED MONOPOLE-QUADRUPOLE MODES OF DENSITY OSCILLATIONS

For completeness, we discuss here the coupled small-amplitude monopole-quadrupole oscillations of density for a BEC confined in a harmonic trap with cylindrical (uniaxial) symmetry, restricting to the case of zero dipole-dipole interaction, $\varepsilon_D=0$. Setting $\omega_z\neq\omega_y=\omega_x=\omega_\perp$ in the eigenvalue problem (116) we easily find analytical expressions for three eigenmodes. First,

$$\Omega^{(0)}_{x^2-y^2}=\sqrt{2}\omega_\perp,\qquad \begin{bmatrix}\widehat{\rho}_{xx}\left(\Omega^{(0)}_{x^2-y^2}\right)\\ \widehat{\rho}_{yy}\left(\Omega^{(0)}_{x^2-y^2}\right)\\ \widehat{\rho}_{zz}\left(\Omega^{(0)}_{x^2-y^2}\right)\end{bmatrix}=\begin{bmatrix}1\\-1\\0\end{bmatrix}.\tag{D1}$$

It follows directly from (81) that this eigenmode corresponds for all anisotropy ratios to a density fluctuation $\delta n_\Omega(\mathbf{r},t)$ with pure $d_{x^2-y^2}$ symmetry:

$$\Omega=\Omega^{(0)}_{x^2-y^2},\quad \delta n_\Omega(\mathbf{r},t)=2n_0\cos\left(\Omega t+\delta_\Omega\right)\frac{r_x^2-r_y^2}{\left[\lambda_\perp^{(0)}\right]^2}.$$

The second and third eigenmodes $\widehat{\rho}_{aa}(\Omega^{(0)}_\pm)$ with eigenfrequencies $\Omega^{(0)}_\pm$ form a doublet consisting of a combination of basis elements with $s$-wave and $d_{z^2}$-wave symmetry. We obtain as a function of the anisotropy ratio $\nu=\frac{\omega_z}{\omega_\perp}$ the following exact results for the eigenfrequencies and the eigenvectors:

$$\Omega^{(0)}_+=\omega_\perp\left[\frac{4+3\nu^2+\sqrt{16-16\nu^2+9\nu^4}}{2}\right]^{\frac{1}{2}},\qquad \begin{bmatrix}\widehat{\rho}_{xx}(\Omega^{(0)}_+)\\ \widehat{\rho}_{yy}(\Omega^{(0)}_+)\\ \widehat{\rho}_{zz}(\Omega^{(0)}_+)\end{bmatrix}=\begin{bmatrix}\frac{4-3\nu^2+\sqrt{16-16\nu^2+9\nu^4}}{4\nu^2}\\ \frac{4-3\nu^2+\sqrt{16-16\nu^2+9\nu^4}}{4\nu^2}\\ 1\end{bmatrix}.\tag{D2}$$

For $\nu\to\infty$ this mode becomes quasi-one-dimensional:

$$\nu\gg1,\qquad \Omega^{(0)}_+=\sqrt{3}\omega_z\left(1+\frac{1}{9\nu^2}+\cdots\right),\qquad \begin{bmatrix}\widehat{\rho}_{xx}(\Omega^{(0)}_+)\\ \widehat{\rho}_{yy}(\Omega^{(0)}_+)\\ \widehat{\rho}_{zz}(\Omega^{(0)}_+)\end{bmatrix}=\begin{bmatrix}\frac{1}{3\nu^2}+\cdots\\ \frac{1}{3\nu^2}+\cdots\\ 1\end{bmatrix},$$

while for $\nu\to0$ it is quasi-two-dimensional:

$$\Omega^{(0)}_+=2\omega_\perp\left(1+\frac{1}{16}\nu^2+\cdots\right),\qquad \begin{bmatrix}\widehat{\rho}_{xx}(\Omega^{(0)}_+)\\ \widehat{\rho}_{yy}(\Omega^{(0)}_+)\\ \widehat{\rho}_{zz}(\Omega^{(0)}_+)\end{bmatrix}=\begin{bmatrix}\frac{2}{\nu^2}-\frac{5}{4}+\cdots\\ \frac{2}{\nu^2}-\frac{5}{4}+\cdots\\ 1\end{bmatrix}.$$

For an anisotropy ratio $\nu \simeq 1$(slightly deformed sphere) the associated density fluctuation $\delta n_\Omega(\mathbf{r},t)$ is of the *breather* type, i.e., a strongly weighted isotropic $s$-wave part is combined with only a small admixture of quadrupolar $d_{z^2}$-wave symmetry:

$$\Omega = \Omega_+^{(0)},$$
$$\delta n_\Omega(\mathbf{r},t) = 2n_0\cos(\Omega t + \delta_\Omega) \times \left[\left(\frac{4-3\nu^2+\sqrt{16-16\nu^2+9\nu^4}}{2\nu^2}+\frac{1}{2}\right)\frac{r_x^2+r_y^2}{[\lambda_\perp^{(0)}]^2} + \left(\frac{4-3\nu^2+\sqrt{16-16\nu^2+9\nu^4}}{4\nu^2}+\frac{3}{2}\right)\frac{r_z^2}{[\lambda_z^{(0)}]^2} - \left(\frac{4-3\nu^2+\sqrt{16-16\nu^2+9\nu^4}}{4\nu^2}+\frac{1}{2}\right)\right]. \quad \text{(D3)}$$

The other eigenmode of the doublet is characterized by

$$\Omega_-^{(0)} = \omega_\perp\left(\frac{4+3\nu^2-\sqrt{16-16\nu^2+9\nu^4}}{2}\right)^{\frac{1}{2}},$$
$$\begin{bmatrix}\widehat{\rho}_{xx}(\Omega_-^{(0)})\\ \widehat{\rho}_{yy}(\Omega_-^{(0)})\\ \widehat{\rho}_{zz}(\Omega_-^{(0)})\end{bmatrix} = \begin{bmatrix}\frac{4-3\nu^2-\sqrt{16-16\nu^2+9\nu^4}}{4\nu^2}\\ \frac{4-3\nu^2-\sqrt{16-16\nu^2+9\nu^4}}{4\nu^2}\\ 1\end{bmatrix}. \quad \text{(D4)}$$

For $\nu \to \infty$ this mode behaves asymptotically as

$$\Omega_-^{(0)} = \sqrt{\frac{10}{3}}\omega_\perp\left(1-\frac{1}{9\nu^2}+\cdots\right),$$
$$\begin{bmatrix}\widehat{\rho}_{xx}(\Omega_-^{(0)})\\ \widehat{\rho}_{yy}(\Omega_-^{(0)})\\ \widehat{\rho}_{zz}(\Omega_-^{(0)})\end{bmatrix} = \begin{bmatrix}-\frac{3}{2}+\frac{5}{3\nu^2}+\cdots\\ -\frac{3}{2}+\frac{5}{3\nu^2}+\cdots\\ 1\end{bmatrix}.$$

For $\nu \to 0$ we find

$$\Omega_-^{(0)} = \sqrt{\frac{5}{2}}\omega_z\left(1-\frac{\nu^2}{16}+\cdots\right),$$
$$\begin{bmatrix}\widehat{\rho}_{xx}(\Omega_-^{(0)})\\ \widehat{\rho}_{yy}(\Omega_-^{(0)})\\ \widehat{\rho}_{zz}(\Omega_-^{(0)})\end{bmatrix} = \begin{bmatrix}-\frac{1}{4}-\frac{5}{32}\nu^2+\cdots\\ -\frac{1}{4}-\frac{5}{32}\nu^2+\cdots\\ 1\end{bmatrix}.$$

For an anisotropy ratio $\nu \simeq 1$ (slightly deformed sphere) this mode describes a density fluctuation with a strongly weighted $d_{z^2}$-wave part and only a small admixture of isotropic $s$-wave symmetry:

$$\Omega = \Omega_-^{(0)},$$
$$\delta n_\Omega(\mathbf{r},t) = 2n_0\cos(\Omega t + \delta_\Omega) \times \left[\left(\frac{4-3\nu^2-\sqrt{16-16\nu^2+9\nu^4}}{2\nu^2}+\frac{1}{2}\right)\frac{r_x^2+r_y^2}{[\lambda_\perp^{(0)}]^2} + \left(\frac{4-3\nu^2-\sqrt{16-16\nu^2+9\nu^4}}{4\nu^2}+\frac{3}{2}\right)\frac{r_z^2}{\lambda_z^2} - \left(\frac{4-3\nu^2-\sqrt{16-16\nu^2+9\nu^4}}{4\nu^2}+\frac{1}{2}\right)\right]. \quad \text{(D5)}$$

The derived frequencies for the coupled monopole-quadrupole oscillations of a BEC without dipole-dipole interaction, i.e., $\varepsilon_D = 0$, that is confined inside a harmonic trap with uniaxial (cylindrical) symmetry, coincide with well-known results first derived by Stringari [19] using a different method, that enabled him also to derive all the higher-lying frequencies.


[1] C. J. Pethick and H. Smith, *Bose-Einstein Condensation in Dilute Gases*, 2nd ed. (Cambridge University Press, New York, 2008).
[2] L. Santos, G. V. Shlyapnikov, P. Zoller, and M. Lewenstein, Phys. Rev. Lett. **85**, 1791 (2000).
[3] T. Lahaye, C. Menotti, L. Santos, M. Lewenstein, and T. Pfau, Rep. Prog. Phys. **72**, 126401 (2009).
[4] M. Vengalattore, S. R. Leslie, J. Guzman, and D. M. Stamper-Kurn, Phys. Rev. Lett. **100**, 170403 (2008).
[5] S. Ospelkaus, A. Pe'er, K.-K. Ni, J. J. Zirnel, B. Neyenhuis, S. Kotochigova, P. S. Julienne, J. Ye, and D. S. Jin, Nat. Phys. **4**, 622 (2008).
[6] K. Chebakov, A. Sokolov, A. Akimov, D. Sukachev, S. Kanorsky, N. Kolachevsky, and V. Sorokin, Opt. Lett. **34**, 2955 (2009).
[7] A. J. Berglund, J. L. Hanssen, and J. J. McClelland, Phys. Rev. Lett. **100**, 113002 (2008).
[8] M. Lu, S. H. Youn, and B. L. Lev, Phys. Rev. Lett. **104**, 063001 (2010).
[9] A. Griesmaier, J. Stuhler, T. Koch, M. Fattori, T. Pfau, and S. Giovanazzi, Phys. Rev. Lett. **97**, 250402 (2006).
[10] C. Eberlein, S. Giovanazzi, and D. H. J. O'Dell, Phys. Rev. A **71**, 033618 (2005).
[11] S. Chandrasekhar, *Lectures in Theoretical Physics* (University of Colorado Press, Boulder, 1964), Vol. VI, pp. 1–72.
[12] D. Guéry-Odelin and S. Stringari, Phys. Rev. Lett. **83**, 4452 (1999).
[13] S. E. Pollack, D. Dries, M. Junker, Y. P. Chen, T. A. Corcovilos, and R. G. Hulet, Phys. Rev. Lett. **102**, 090402 (2009).
[14] T. Koch, T. Lahaye, J. Metz, B. Fröhlich, A. Griesmaier, and T. Pfau, Nat. Phys. **4**, 218 (2008).
[15] S. E. Pollack, D. Dries, R. G. Hulet, K. M. F. Magalhaes, E. A. L. Henn, E. R. F. Ramos, M. A. Caracanhas, and V. S. Bagnato, Phys. Rev. A **81**, 053627 (2010)
[16] I. Sapina, T. Dahm, and N. Schopohl (unpublished).
[17] O. M. Marago, S. A. Hopkins, J. Arlt, E. Hodby, G. Hechenblaikner, and C. J. Foot, Phys. Rev. Lett. **84**, 2056 (2000).
[18] M. Cozzini, S. Stringari, V. Bretin, P. Rosenbusch, and J. Dalibard, Phys. Rev. A **67**, 021602(R) (2003).
[19] S. Stringari, Phys. Rev. Lett. **77**, 2360 (1996).
[20] O. Bohigas, A. M. Lane, and J. Martorell, Phys. Rep. **51**, 267 (1979).
[21] S. Giovanazzi, L. Santos, and T. Pfau, Phys. Rev. A **75**, 015604 (2007).
[22] B. C. Carlson, Numer. Math. **33**, 1 (1979).
[23] W. H. Press, S. A. Teukolsky, W. T. Vetterling, and B. P. Flannery, *Numerical Recipes in C* (Cambridge University Press, New York, 1992).
[24] R. M. W. van Bijnen *et al.*, Phys. Rev. A **82**, 033612 (2010).